AGU PUBLICATIONS

JGR

Journal of Geophysical Research: Oceans

RESEARCH ARTICLE

10.1002/2017JC013490

Assimilation of Ocean-Color Plankton Functional Types to Improve Marine Ecosystem Simulations

S. Ciavatta[1,2], R. J. W. Brewin[1,2], J. Skákala[1,2], L. Polimene[1], L. de Mora[1], Y. Artioli[1], and J. I. Allen[1,2]

[1]Plymouth Marine Laboratory, Plymouth, UK, [2]Plymouth Marine Laboratory/National Centre for Earth Observation, Plymouth, UK

Key Points:
- Assimilation of phytoplankton functional types improved the simulation of the plankton community structure
- The simulation of CO_2 partial pressure was improved, impacting the estimate of the air-sea carbon flux
- Assimilation of phytoplankton functional types outperformed that of total chlorophyll

Supporting Information:
- Supporting Information S1

Correspondence to:
S. Ciavatta,
s.ciavatta@pml.ac.uk

Citation:
Ciavatta, S., Brewin, R. J. W., Skákala, J., Polimene, L., de Mora, L., Artioli, Y., & Allen, J. I. (2018). Assimilation of ocean-color plankton functional types to improve marine ecosystem simulations. *Journal of Geophysical Research: Oceans*, *123*. https://doi.org/10.1002/2017JC013490

Received 26 SEP 2017
Accepted 28 DEC 2017
Accepted article online 19 JAN 2018

Abstract We assimilated phytoplankton functional types (PFTs) derived from ocean color into a marine ecosystem model, to improve the simulation of biogeochemical indicators and emerging properties in a shelf sea. Error-characterized chlorophyll concentrations of four PFTs (diatoms, dinoflagellates, nanoplankton, and picoplankton), as well as total chlorophyll for comparison, were assimilated into a physical-biogeochemical model of the North East Atlantic, applying a localized Ensemble Kalman filter. The reanalysis simulations spanned the years 1998–2003. The skill of the reference and reanalysis simulations in estimating ocean color and in situ biogeochemical data were compared by using robust statistics. The reanalysis outperformed both the reference and the assimilation of total chlorophyll in estimating the ocean-color PFTs (except nanoplankton), as well as the not-assimilated total chlorophyll, leading the model to simulate better the plankton community structure. Crucially, the reanalysis improved the estimates of not-assimilated in situ data of PFTs, as well as of phosphate and pCO_2, impacting the simulation of the air-sea carbon flux. However, the reanalysis increased further the model overestimation of nitrate, in spite of increases in plankton nitrate uptake. The method proposed here is easily adaptable for use with other ecosystem models that simulate PFTs, for, e.g., reanalysis of carbon fluxes in the global ocean and for operational forecasts of biogeochemical indicators in shelf-sea ecosystems.

1. Introduction

Shelf-sea ecosystems are crucial to humankind, because they provide ~20% of the marine primary production (Jahnke, 2010), ~20% of the global ocean uptake of atmospheric carbon dioxide (CO_2) (Borges, 2011), and over 90% of the global fish catches (Pauly et al., 2002). Improved understanding and simulation of biogeochemical indicators and fluxes in shelf-seas can be achieved by merging marine ecosystem models and ocean-color data using assimilation algorithms (Ciavatta et al., 2011). These algorithms correct the model prediction toward the observations, with the goal of improving the biogeochemical estimates obtained separately from monitoring and modeling (Lahoz & Schneider, 2014).

The satellite ocean-color product typically assimilated into marine models is total chlorophyll concentration (Gehlen et al., 2015). In general, this significantly improves the model simulation of total chlorophyll itself. However, it may also degrade the simulation of not-assimilated biogeochemical variables (see discussions in Ford & Barciela, 2017; Gregg et al., 2009; Teruzzi et al., 2014; Tsiaras et al., 2017) and the advantages of assimilating alternative ocean-color products have been explored, e.g., optical properties (Ciavatta et al., 2014; Jones et al., 2016; Shulman et al., 2013) and particulate organic carbon (Xiao & Friedrichs, 2014a, 2014b).

Total chlorophyll is linked to the density of the phytoplankton community as a whole (Sathyendranath et al., 1989), however, the size of the phytoplankton groups composing the community plays a key role in marine ecology and biogeochemical cycling, because the size impacts growth, nutrient assimilation, sinking rate, and predation (Chisholm, 1992). State-of-the-art models describe size-based phytoplankton functional types (PFTs) to increase the realism of marine ecosystem simulations (a nonexhaustive list of such models includes ERSEM (Baretta et al., 1995; Butenschön et al., 2016; PISCES, Aumont et al., 2003; NOBM, Gregg et al., 2003; BFM, Vichi et al., 2007; the MITgcm-biogeochemical model, Follows et al., 2007; PlankTOM, Le Quéré et al., 2005; and MEDUSA, Yool et al., 2013). However, the simulation of phytoplankton types remains challenging, due mainly to the difficulty of formulating their processes (Shimoda & Arhonditsis, 2016), and the assimilation of total chlorophyll has not resolved this issue (Ciavatta et al., 2011).

Xiao and Friedrichs (2014a, 2014b) showed that assimilation of size-fractionated chlorophyll for off-line parameter optimization improved the simulation of plankton groups with testbed one-dimensional models of the mid-Atlantic Bight. The recent production of error-characterized ocean-color estimates of four plankton functional types for the North West European Shelf (Brewin et al., 2017) provides an opportunity to investigate the impact of their sequential assimilation into a three-dimensional model of this region (Ciavatta et al., 2016), where PFT simulation remains challenging (Ford et al., 2017).

The overarching objective of this work is to test whether the simulation of the North-West European shelf-sea ecosystem can be improved by assimilating ocean-color products of plankton functional types into a marine model. The specific objectives of this manuscript are: (1) to assess the skill of PFT assimilation in estimating biogeochemical data, also in comparison to total chlorophyll assimilation; (2) to illustrate the emergence of ecosystem properties driven by PFT assimilation. In this context, emergent properties are ecosystem features that are not prognostic variables included in the model equations (de Mora et al., 2016) and in the multivariate assimilative analysis. Here we discuss how PFTs assimilation drives: (a) changes in the representation of the plankton community structure; and (b) changes in the simulated uptake of atmospheric CO_2 by the shelf-sea ecosystem.

To achieve the objectives, we assimilated a regional ocean-color product for plankton functional types (Brewin et al., 2017) into an assimilative modeling system of the North East Atlantic (Ciavatta et al., 2016). This system was developed by Ciavatta et al. (2016) to provide the first decadal reanalysis of biogeochemical indicators and fluxes in the North West European shelf, by assimilating concentrations of total chlorophyll. This system has been upgraded here to the state-of-the-art version and parameterization of the European Regional Seas Ecosystem Model (ERSEM) (Butenschön et al., 2016) and its assimilation algorithm (i.e., the Ensemble Kalman filter, Ciavatta et al., 2016; Evensen, 1994) has been adapted to the simultaneous assimilation of the chlorophyll concentrations of four PFTs. This assimilation system was applied in the reanalysis of the biogeochemistry of the North West European shelf in the years 1998–2003. The output was skill-evaluated using ocean-color products and in situ observations of 14 physical and biogeochemical variables.

The paper is structured as follows. Section 2 describes the ecosystem model, the set-up of the assimilation algorithm, the data, and the metrics applied for skill evaluation. The results are presented in section 3, where the skill of the reanalysis is evaluated by using the assimilated PFT and the not-assimilated total chlorophyll ocean-color products (section 3.1), and then by using a not-assimilated in situ data set (section 3.2). The results are discussed in section 4, by illustrating the assimilative impact on the simulation of emerging properties of the ecosystem, i.e., the structure of the plankton community (section 4.1) and the biogeochemical fluxes influencing the reanalysis skill (section 4.2). Concluding remarks and future applications are pointed out in section 5.

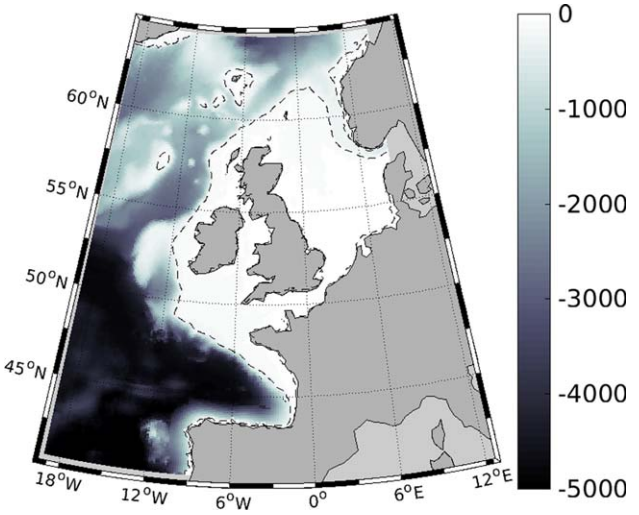

Figure 1. Bathymetry (m) of the North East Atlantic region represented in the model domain. The dashed lines represent the 200 m isobath delimiting the North West European shelf and the 10 m isobath delimiting the shallowest areas.

2. Material and Methods

2.1. The Ecosystem Model of the North East Atlantic

The ecosystem dynamics of the North East Atlantic, including the North West European shelf, (Figure 1) are described by a three-dimensional physical-biogeochemical model (Artioli et al., 2012; Wakelin et al., 2012).

The model consists of three on-line coupled submodels (see Figure 2): the Proudman Oceanographic Laboratory Coastal Ocean Modelling System (POLCOMS) (Holt & James, 2001), which describes the hydrodynamics and provides the physical forcing to the pelagic biogeochemical submodel, namely the European Regional Seas Ecosystem Model (ERSEM) (Baretta et al., 1995; Butenschön et al., 2016). The third submodel is the ERSEM benthic biogeochemical model (Blackford, 1997; Butenschön et al., 2016). The submodels are coupled at the same temporal and spatial resolution as the physical model, to capture the effects of the three-dimensional hydrodynamics on the biogeochemical cycles (Holt et al., 2004). The grid of the

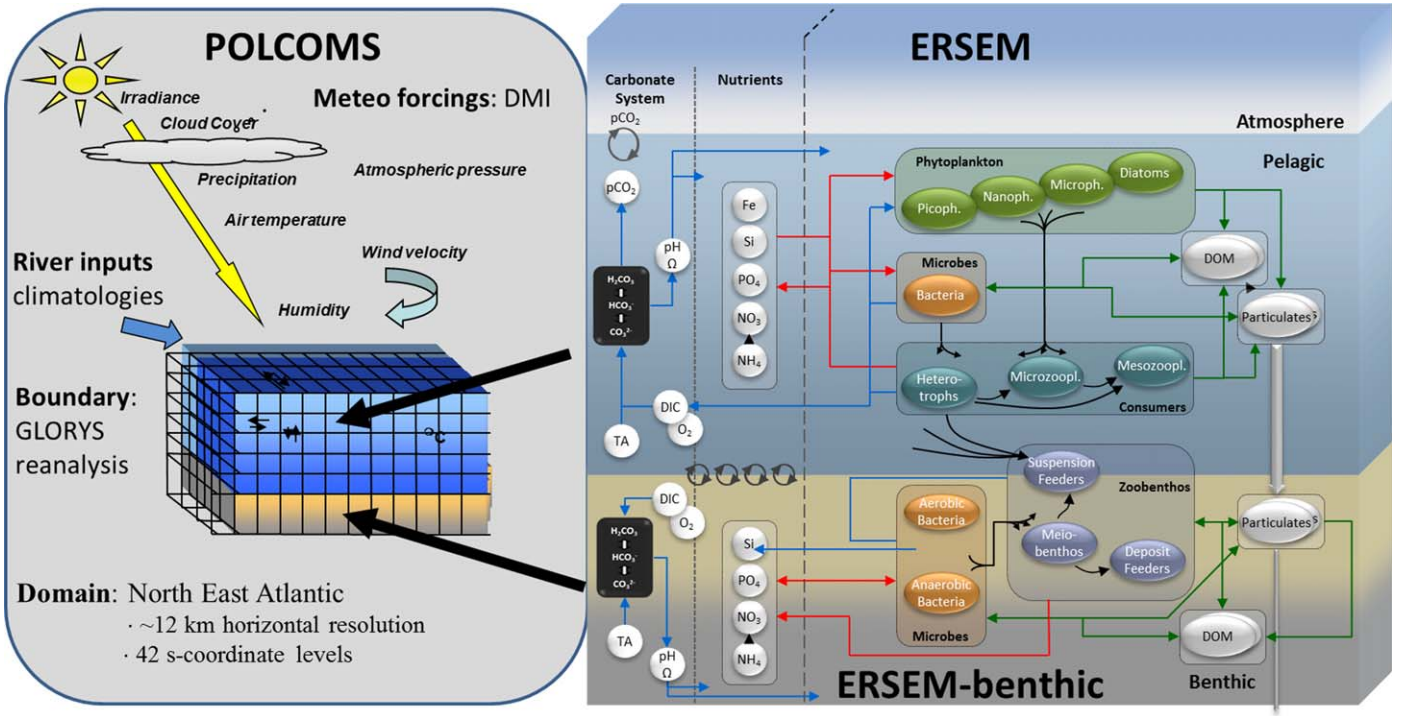

Figure 2. Schematic of the ecosystem model coupling the physical submodel POLCOMS and the pelagic and benthic biogeochemical submodels of ERSEM.

model spatial domain has a horizontal resolution of 1/6° in longitude and 1/9° in latitude, approximating to ~12 km at the latitude of the study region, and it has 42 s-coordinate levels in the vertical (Wakelin et al., 2012).

2.1.1. The Physical Submodel: POLCOMS

The physical model POLCOMS (Holt & James, 2001) is a three-dimensional baroclinic, finite-difference, primitive equation model formulated in spherical-polar coordinates on an Arakawa B-grid. Both temperature and salinity are treated as prognostic variables. The model includes: an advection scheme with stability and conservation properties (James, 1996); a vertical turbulence model (GOTM) (Burchard et al., 1999); and calculation of horizontal pressure gradients.

2.1.2. The Pelagic Biogeochemical Submodel: ERSEM

The biogeochemical dynamics are described by the European Regional Seas Ecosystem model (ERSEM) (Baretta et al., 1995), here applied using a configuration with 51 pelagic variables and the recent parameterization by Butenschön et al. (2016). In a supplementary numerical experiment, we applied the model also with the previous parameterization by Blackford et al. (2004) (Appendix A). ERSEM uses a functional type approach to model the dynamics of the low trophic levels of the ecosystem. Primary producers are split into four phytoplankton functional types (PFTs), including three size-based types (picophytoplankton, nanophytoplankon, and microphytoplankton), plus diatoms as silicate users. Each of these PFTs is represented in terms of its content of chlorophyll, carbon, nitrogen, phosphate, and (for diatoms only) silicate. Three functional types of zooplankton (mesozooplankton, microzooplankton, and heterotrophic nanoflagellates) prey on the PFTs, bacteria, and particulate organic matter as a function of their size. A bacterial functional type drives the microbial loop, the production, and recycling of dissolved organic matter in labile and recalcitrant forms, and it drives the regeneration of inorganic nutrients in the water column (Hansell, 2013; Polimene et al., 2006). In the functional types, the stoichiometric ratios of nutrients-to-carbon and chlorophyll-to-carbon (in the PFTs) vary dynamically (Baretta-Bekker et al., 1997; Geider et al., 1997). The model simulates the dynamics of five inorganic dissolved nutrients (carbon, nitrate, ammonium, phosphate, and silicate), and dissolved oxygen. Nitrogen undergoes nitrification in the water column, as a function of available ammonium, temperature, oxygen, and pH (Blackford & Gilbert, 2007; Butenschön et al., 2016). Denitrification is assumed to be negligible in the shelf pelagic environment and is modeled in the sediments only. The model configuration applied here includes a carbonate system module, which regulates the air-sea flux

of carbon dioxide, as well as the description of calcite, including its deposition at the sea floor (Artioli et al., 2012; Butenschön et al., 2016).

Numerous works demonstrated the skill of ERSEM in representing processes, emerging properties, and observations in marine ecosystems (e.g., Allen & Somerfield, 2009; Butenschön et al., 2016; de Mora et al., 2013, 2016; Saux-Picart et al., 2012). However, the model can have low skill in representing observed phytoplankton successions (in particular blooms of dinoflagellates) in shelf-sea applications, due to limitations in the parameterization of the PFTs (Blackford et al., 2004; Ciavatta et al., 2011, 2016; Ford et al., 2017) that have been addressed by Butenschön et al. (2016). The differences in the PFT parameters applied here and in the previous assimilation system of the North East Atlantic (Ciavatta et al., 2016) are listed in supporting information Table S1.

2.1.3. The ERSEM Benthic Submodel

The benthic submodel is the ERSEM benthic model (Blackford, 1997), as described in Butenschön et al. (2016). In the configuration applied here, the submodel includes 35 biogeochemical variables, subdivided into five living functional types (including three zoobenthos types, and aerobic and anaerobic bacteria), along with particulate matter and dissolved organic and inorganic nutrients. The fluxes at the sediment-water interface are determined by sedimentation and diffusion of inorganic material across the seabed.

2.1.4. Boundary Conditions and Atmospheric Forcing

The model simulation was setup as in Ciavatta et al. (2016). The oceanic conditions at the open boundaries of the ecosystem model (temperature, salinity, currents, and sea surface elevation) were extracted for the years 1998–2003 from the GLORYS reanalysis product provided within the EC FP7 project MyOcean (Ferry et al., 2012). The corresponding conditions for dissolved nutrients and oxygen were extracted from the 2005 World Ocean Atlas climatology (Garcia et al., 2006a, 2006b), and for dissolved inorganic carbon (DIC) from the database GLODAP (Key et al., 2004).

The model is forced by daily climatological discharges of freshwater and dissolved nutrients from 250 rivers. Data of water discharge were taken from the Global River Discharge Data Base (Vörösmarty et al., 1996), and from data prepared by the UK Centre for Ecology and Hydrology. River nutrient loadings match those used by Lenhart et al. (2010), with raw data for the UK, Northern Ireland, Ireland, France, Norway, Denmark, and the Baltic processed by the UK Centre for Environment Fisheries and Aquaculture Science, and raw data for Germany and the Netherlands derived from Pätsch and Lenhart (2004). In addition, Baltic inflow was represented as river-inflow (Wakelin et al., 2012). Atmospheric input of nutrients was derived from the European Monitoring and Evaluation Programme (Tørseth et al., 2012).

The atmospheric forcing (3 hourly solar irradiation, air temperature, wind velocity, precipitation, humidity, pressure, and cloud cover), was obtained from a regional climate hindcast (years 1989–2009, spatial resolution of 12 km) performed by the Danish Climate Centre, using the regional Climate model HIRHAM5 (Christensen et al., 2006), driven by ERA-interim global reanalysis (Dee et al., 2011).

2.2. The Assimilation System

The assimilation system is described in full in Ciavatta et al. (2016). It uses the Ensemble Kalman filter (EnKF) (Evensen, 1994). This is a sequential assimilation method, which starts by randomly sampling an ensemble of N state vectors $\mathbf{x}_0^{a(l)}$ (l = 1, 2, . . ., N) from an initial probability density function for the model variables. Each ensemble member, i.e., state vector, is propagated in time using the nonlinear model equations during the "forecast step," that provides the EnKF "forecasts" $\mathbf{x}_i^{f(l)}$.

At time i, the forecast state $\mathbf{x}_i^f$ and the forecast uncertainty $\mathbf{P}_i^f$ are defined from the mean value and the covariance matrix of the N forecasted members. When at time i a vector $\mathbf{y}_i^o$ of observations of the model output $\mathbf{y}_i = \mathbf{H}[\mathbf{x}_i^{f(l)}]$ becomes available, the assimilation scheme updates (i.e., "corrects") the forecasted states $\mathbf{x}_i^{f(l)}$, in the EnKF "analysis" step. This step scales the forecast-to-data mismatches, by balancing the uncertainty in the model ($\mathbf{P}_i^f$) and in the observations ($\mathbf{R}_i$) and it provides the analyzed ensemble $\mathbf{x}_i^{a(l)}$. The difference $\mathbf{x}_i^{a(l)}$-$\mathbf{x}_i^{f(l)}$ is the "increment" (i.e., the correction) of the state vector in the analysis step. The ensemble $\mathbf{x}_i^{a(l)}$ is the initial condition used to simulate a new ensemble forecast for time $i + 1$, in a sequential procedure that estimates the evolution of the model variables over the time window spanned by the assimilated data.

Our assimilation system uses the Evensen (2003) version of the EnKF, which includes localization of the analysis and perturbation of the assimilated observations (see also Hu et al., 2012; Natvik & Evensen, 2003;

Storto et al., 2013). Observations and model states are log-transformed prior to the analysis, to guarantee positivity of the solutions (Janjić et al., 2014), as in the applications by Torres et al. (2006), Nerger and Gregg (2007), and Ciavatta et al. (2011, 2014, 2016).

The only difference in the EnKF system implemented here with respect to Ciavatta et al. (2016) is the definition of the observational operator $\mathbf{H}\left[\mathbf{x}_i^{f(l)}\right]$. Here the operator links the four state variables representing the ERSEM plankton types to the respective data, rather than linking total chlorophyll data to the corresponding ERSEM diagnostic variable (i.e., the sum of the four chlorophyll types) included in the augmented state vector.

2.2.1. Setup of the Assimilation Scheme

The setup of the assimilation scheme is the same by Ciavatta et al. (2016). We used the EnKF with an ensemble size of $N = 100$ members. To keep the analysis affordable computationally, the analyzed state vector had to include a maximum of 44 out of the 51 biogeochemical state variables. The remaining seven variables (silicate in dissolved, medium-particulate and large-particulate forms, semilabile dissolved organic carbon, dissolved oxygen, alkalinity, and calcite) were excluded because were more likely to create instabilities in the reanalysis and were updated through the model equation during the simulation runtime ("forecast" step) (Ciavatta et al., 2016) The radius of the localized analysis was set spatially variable as a function of the bathymetry. In particular, we increased the "resolution" of the analysis from oceanic toward coastal waters, by setting a radius of 100 km for grid points where the bathymetry is deeper than 2,000 m (i.e., in 35% of the cells of the model grid), 50 km for bathymetry between 50 and 2,000 m (51% of the grid), and 25 km for bathymetry shallower than 50 m (14% of the grid) (Ciavatta et al., 2016).

Model error is accounted for by random perturbations of the model forcing, namely the surface solar irradiance, thus inducing fluctuations in the underwater light field that drives photosynthesis (Ciavatta et al., 2016). A Gaussian perturbation with standard deviation equal to 20% of the irradiance value is added during the model forecast step. Furthermore, at the first assimilation step of each year, model error is added to all the variables undergoing the analysis, as white noise drawn from a distribution of pseudorandom fields with error equal to 10% of the value of the variables. The error is lowered to 1% for those variables that have relatively high mean values (DIC, ammonium, small particulate matter), to avoid divergences in the concentrations of the largest pool in the model (Ciavatta et al., 2011).

The ensemble was initialized by perturbing the output of a hindcast model simulation that started in January 1991 after a 5 year spin-up. The hindcast states for September 1997 were perturbed by using Gaussian pseudorandom fields with error equal to 30% of the value of the variables. These perturbed states were used to start the assimilation from the first data available in the ocean color time series.

The observational error of the PFTs concentrations was computed from the per-pixel root-mean-square-deviation provided by the TOSCA ocean color product (Brewin et al., 2017). The variance of the unbiased PFT concentrations regridded onto the surface model domain was computed following the procedure described in the Appendix A of Ciavatta et al. (2016).

The reanalysis simulation was run on the UK NERC High Performance Computing facility "ARCHER," using 7200 CPUs and $\sim$9 Mega Allocation Units (MAUs).

2.3. Data

The ocean-color chlorophyll concentration of phytoplankton functional types used in the assimilation (Figure 3) were provided by the project TOSCA ("Towards Operational Size-class Chlorophyll Assimilation") of the Copernicus Marine Environment Monitoring Service (CMEMS) of the European Commission (Brewin et al., 2017). In turn, TOSCA used the global total chlorophyll product provided by the Ocean Color-Climate Change Initiative project of the European Space Agency (ESA's OC-CCI product, Version 3.0; Mélin et al., 2017) and Sea Surface Temperature (SST) data (OISST Version 2.0; Reynolds et al., 2007) acquired from NOAA (http://www.esrl.noaa.gov/psd/data/gridded/data.noaa.oisst.v2.highres.html). The TOSCA data set contains daily values of concentrations of four PFTs (diatoms, dinoflagellates, nanoplankton, and picoplankton) and associate errors (bias and root-mean-square deviations) in the North East Atlantic, at 4 km resolution, spanning the years 1997–2015. Brewin et al. (2017) obtained the PFT concentrations by retuning and modifying a global abundance-based algorithm (Brewin et al., 2010, 2015), to first estimate the chlorophyll concentration of three phytoplankton size-classes (pico [<2 μm], nano [2–20 μm], and microplankton [>20

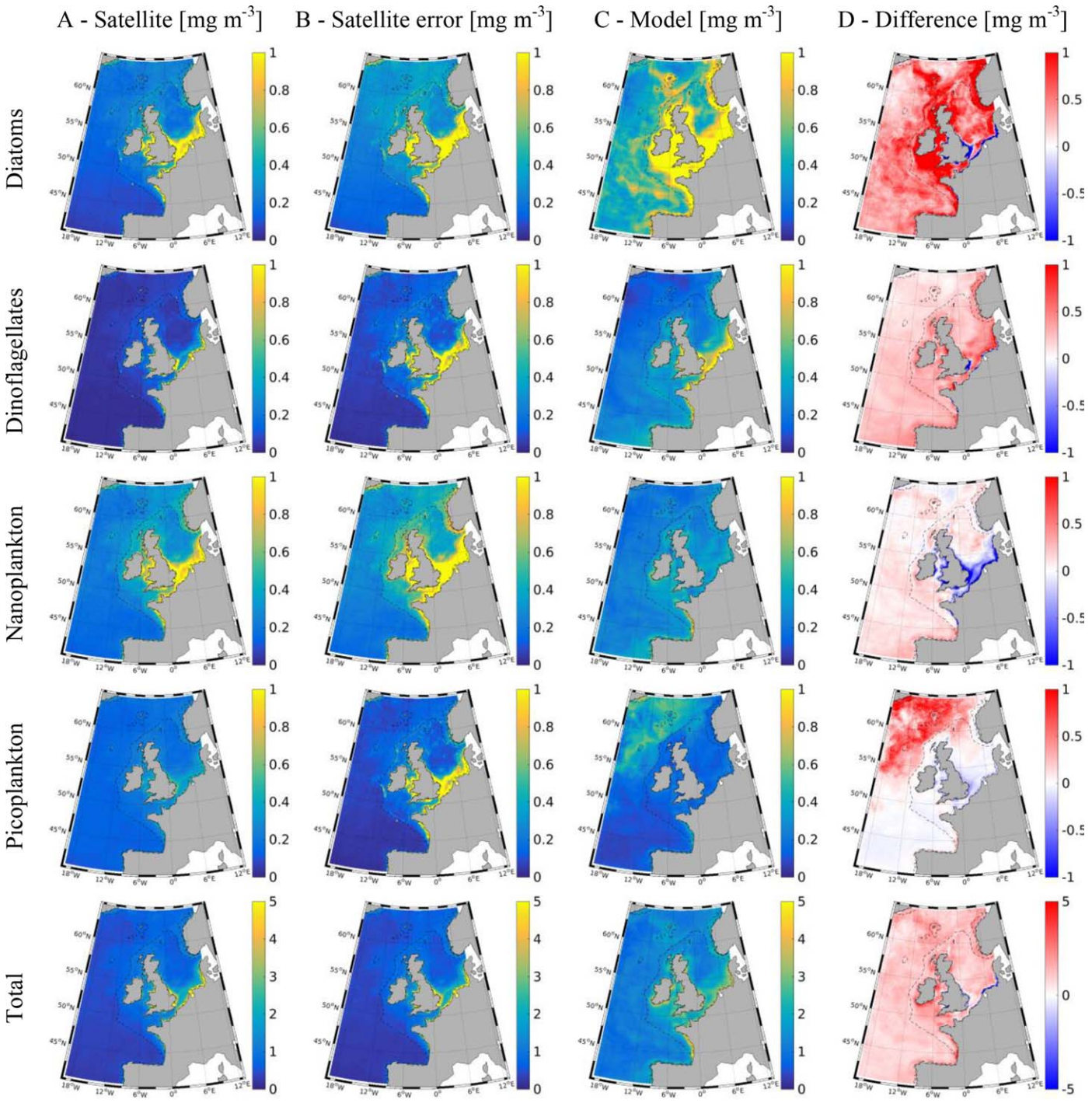

Figure 3. Chlorophyll concentrations of the four phytoplankton types and of total phytoplankton, derived from satellite ocean-color, and from the reference model simulation: mean values in 1998–2003. Column (a) satellite product; (b) nominal standard error of the satellite product; (c) reference model output; and (d) difference between reference model output and satellite product. The dashed lines in the maps represent the 10 and 200 m isobaths.

μm]), accounting for the influence of SST on the model parameters. Microplankton chlorophyll was then partitioned into diatoms and dinoflagellates as a function of SST, tuned specifically to the region, so that the phytoplankton groups provided by the remote-sensing algorithm matched those used in ERSEM (Brewin et al., 2017). For additional details on the satellite algorithm, the reader is referred to section 2.6 and 2.7 of Brewin et al. (2017). The PFT errors were estimated following the approach applied in the ESA's

OC-CCI project (Jackson et al., 2017), i.e., by using a PFT validation data set of satellite and in situ match-ups, and an optical classification of pixels with fuzzy-logic statistics (Moore et al., 2009). Using the same methods applied in Ciavatta et al. (2016) with OC-CCI total chlorophyll, here we computed unbiased concentrations and associated standard errors of the PFT concentrations (Figure 3). These were then projected onto the ~12 km model grid, and daily values were merged into 5 day composites, one for each month in 1998–2003, and centered on the last day of each month. These composites were assimilated in the reanalysis spanning years 1998–2003.

The in situ data used to evaluate the reanalysis skill were measured in the North East Atlantic in the years 1998–2003 and were extracted from the Ecosystem Data Online Warehouse of the International Council for the Exploration of the Sea (www.ices.dk) for the following variables: temperature, salinity, dissolved oxygen, chlorophyll, nitrate, ammonium, phosphate, silicate, and pH. Data of partial pressure of carbon dioxide (pCO_2) were derived from the Surface Ocean CO2 Atlas (synthesis product, version 2; http://www.socat.info) (Bakker et al., 2014). We used also the in situ observations of chlorophyll concentrations of plankton types assembled in TOSCA for the North East Atlantic (overall comprising 2971 HPLC data and 263 size-fractionated fluorometric chlorophyll data available in the years 1998–2003), though they were used to either calibrate or validate the regional PFT ocean color product assimilated here (Brewin et al., 2017).

2.4. Skill Metrics

The assessment of the assimilation skill followed the procedure in Ciavatta et al. (2016). The performance of the reference and reanalysis output (y) in matching the assimilated composites of ocean-color PFT concentrations (y'_c) was evaluated by computing and comparing maps of the root mean square deviation (RMSD) between the time series of y and y'_c at each surface grid point of the model domain. The skill of the reanalysis was evaluated for the output of both the forecast and analysis steps of the assimilation algorithm (see section 2.2 for the definition of these steps).

Quantitative metrics to evaluate the skill of the reanalysis in matching the in situ PFT and biogeochemical data were computed using an open source tool for model validation (https://github.com/bcdev/opec-tools) based on de Mora et al. (2013). Daily values of the variables in the reanalysis data set (y) were matched-up point-to-point in space and time with the data (o). Following the recommendations of Butenschön et al. (2016) and Ciavatta et al. (2016) for the evaluation of the model and data-sets applied here, we computed "robust" skill metrics based on the percentiles and ranks of the distributions, which are less affected by non-gaussianity and outliers than parametric statistics (e.g., Daszykowski et al., 2007) used, e.g., in classical Target Diagrams (Jolliff et al., 2009). In particular, we computed then represented in robust skill diagrams (Butenschön et al., 2016): the bias calculated as the median value of the reanalysis-to-observation mismatch, $bias^* = \text{median}(y\text{-}o)$, normalized by the interquartile range of the data (IQR_o); the unbiased median absolute error, $MAE' = \text{median}\{\text{abs}[y\text{-}o\text{-}bias^*]\}$, normalized by IQR_o, and taken with the algebraic sign of the differences between the interquartile range of the output and the data, sign(IQR- IQR_o); the Spearman rank correlation coefficient. In this diagrams, the closer the point to the center, the lower is the error of the simulation (i.e., the median bias and the unbiased absolute error).

The skill metrics were computed by subdividing the study region in five areas: (i) coastal waters (model bathymetry shallower than 10 m); (ii) upper shelf-waters (bathymetry between 10 and 200 m and water depth above 50 m); (iii) deeper shelf-waters (bathymetry between 10 and 200 m and depth below 50 m); (iv) upper ocean-waters (bathymetry deeper than 200 m and depth above 50 m); and (v) deeper ocean-waters (bathymetry deeper than 200 m and depth below 50 m). In the Results, we present figures relative to the upper shelf-waters area, which includes the largest part of the available in situ observations and is the focus of this work. The figures relative to the remaining areas are presented in the supporting information, for completeness.

2.5. Benchmarking Simulations

The skill of the assimilation of PFT ocean-color product (reanalysis for 1998–2003) was compared to the skill of three additional simulations. The first one is a reference model simulation, without assimilation, for years 1998–2003 (see Figure 3). The second one is a 1998–2003 simulation assimilating concentrations of total chlorophyll, which were derived from the same ESA's OC-CCI product used to derive the plankton functional types (sections 2.3). The same product of total chlorophyll was assimilated in the third simulation, but in

this case we used the ERSEM parameterization of the PFTs by Blackford et al. (2004), rather than the newer parameterization of Butenschön et al. (2016), and the run covered year 1998 only (see Appendix A). Besides the differences we mentioned here, the three additional simulations were identical in using the same setup applied in the PFT assimilative reanalysis.

3. Results

3.1. Skill in Matching the Ocean Color Products

The reanalysis was capable of reproducing the differences in magnitude and distributions of the four phytoplankton functional types (Figure 4) that were observed in the North East Atlantic in the years 1998–2003 (Figure 3). Diatoms and nanoplankton were the dominant groups in both the satellite product and reanalysis output, though the reanalysis overestimated markedly the concentrations of diatoms (see the high RMSD values in Figure 4). Picoplankton and dinoflagellates had lower concentrations, though the last group was noticeably overestimated by the reanalysis. In general, the satellite product and output were consistent in estimating decreasing gradients of the biomass from the coast toward the open ocean. However, diatoms and dinoflagellates dominance extended further offshore in the reanalysis. On the contrary, the observed high coastal concentrations of nanoplankton were underestimated by the assimilative output. The reanalysis of picoplankton was particularly skilled on the shelf and in the southern part of the domain, but it overestimated the satellite-derived concentrations in the Northern region. Overall, the reanalysis provided an estimation of the total phytoplankton community (i.e., total chlorophyll concentration, last row in Figure 4), which is consistent with the magnitude and spatial gradients estimated by the satellite algorithm (Figure 3), though the concentrations remained overestimated.

The reanalysis outperformed the reference model simulation in estimating not only the assimilated plankton functional types, but also the not-assimilated total chlorophyll (column c in Figure 4). In general, the reference model simulation overestimated the PFTs on the ocean and shelf regions, in particular diatoms and picoplankton in the Northern region (see column d in Figure 3). The reanalysis reduced the overestimation by systematically correcting the PFTs toward the lower observed concentrations, reducing the model RMSD up to 50% for dinoflagellates. The reanalysis improved the model estimation of nanoplankton on the shelf, though this was deteriorated on the ocean part of the domain. In most of the domain, the reanalysis improved the estimation of total chlorophyll, though it was not assimilated directly, as a consequence of the improved simulation of the single components of the plankton community.

The assimilation of the PFTs outperformed the assimilation of total chlorophyll not only in estimating the plankton types, but also in the estimating total chlorophyll (column d in Figure 4). The magnitude and spatial patterns of the RMSD changes resemble those relative to the reference simulation (column c), though RMSD improvements were particularly noticeable for picoplankton in the shelf area (column d).

The skill metrics relative to the 1 month "forecasts" produced in the PFTs reanalysis (Figure 5) are substantially coherent to the ones relative to the "analysis" in Figure 4. Improvements of the RMSD are smaller in magnitude and spatial coverage if compared to the analysis, but the forecasts still outperformed the reference simulation and total chlorophyll assimilation. The most evident exception are the forecasts of diatoms, which were less skilled in the North Sea, thus tempering the forecast improvements for total chlorophyll in that area.

3.2. Skill in Matching the In Situ Data

In general, the assimilation of ocean-color PFTs was skilled in estimating the in situ data of PFTs and physical and biogeochemical variables in the upper shelf-waters in the years 1998–2003 (Figures 6 and 7). The output captured qualitatively the central position and dispersion of most of the observations, for most of the variables (Figure 6). The reanalysis-to-observation match-ups are well aligned along the bisector line of the plots for temperature, salinity, and dissolved oxygen, indicating a skilled representation of both the magnitude and variability of the observations. However, salinity and oxygen tended to be underestimated in the reanalysis. The bulk of the match-ups for the partial pressure of CO_2 overlaps or approaches the bisector line, though the reanalysis tended to underestimate (overestimate) low (high) pCO_2 data. Also the area of highest density of phosphate match-ups overlaps the bisector line, though there are several model spikes. Silicate and nitrogen were substantially overestimated by the reanalysis, while ammonium was underestimated. Interestingly, in

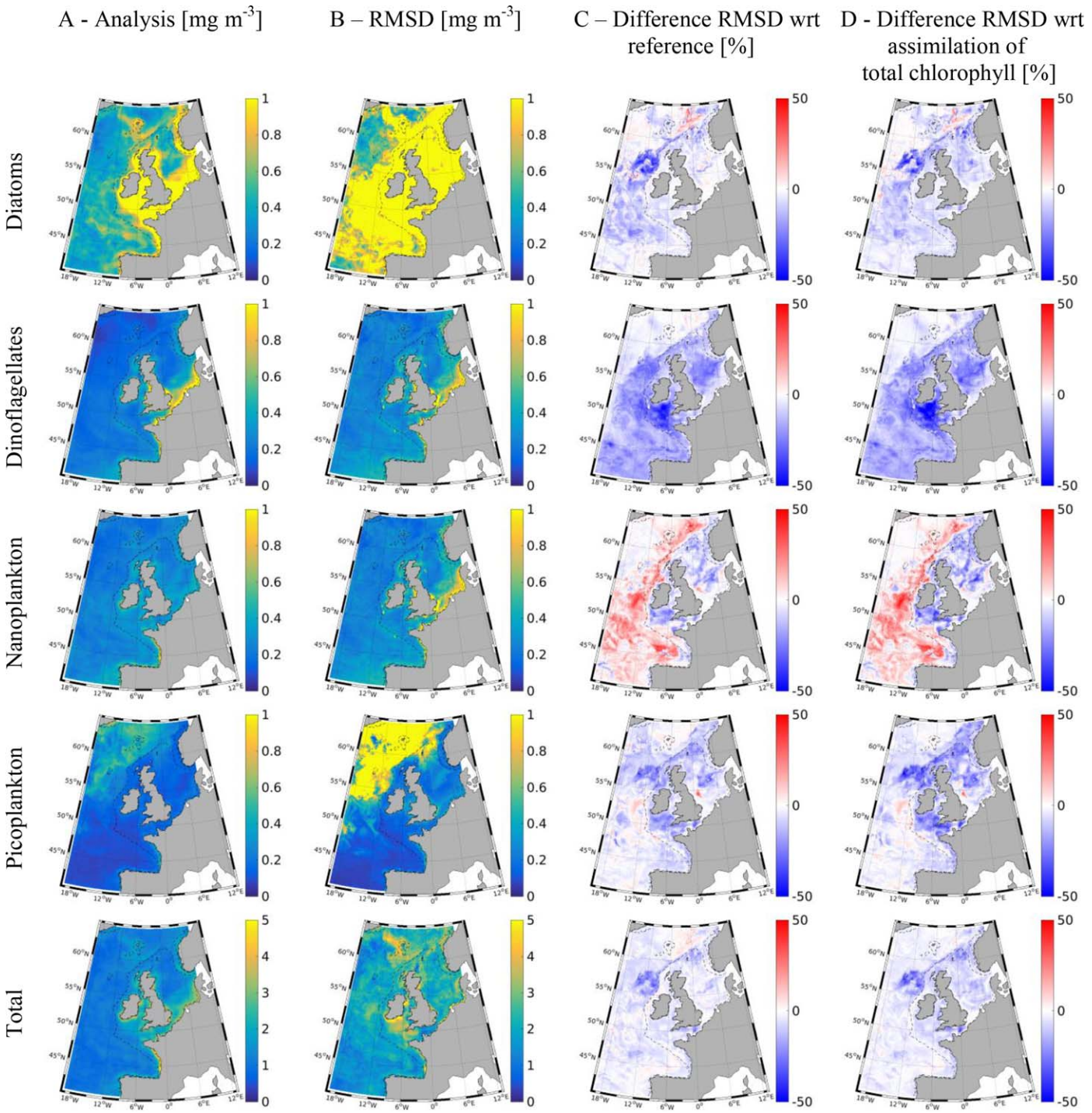

Figure 4. Skill of the PFT assimilation (analysis) in estimating the ocean-color chlorophyll concentrations of the four phytoplankton types and of total phytoplankton: means in 1998–2003. Column (a) output of the PFT assimilative simulation; (b) root-mean-square-deviation (RMSD) between analyses and ocean-color product; (c) percentage difference between the RMSD of the PFT assimilation and of the reference model without assimilation; and (d) percentage difference between the RMSD of the PFT assimilation and of the total chlorophyll assimilation.

the plots of nutrients, two areas of elevated data density are distinguishable at low and high concentrations, representing the summer and winter conditions, respectively, which, in turn, are related to the seasonal cycle of primary production and water-column stratification. Nutrient seasonality is captured by the reanalysis, though the low summer observations were largely overestimated. The reanalysis was able to represent the magnitude of the pH data, but not their fluctuations.

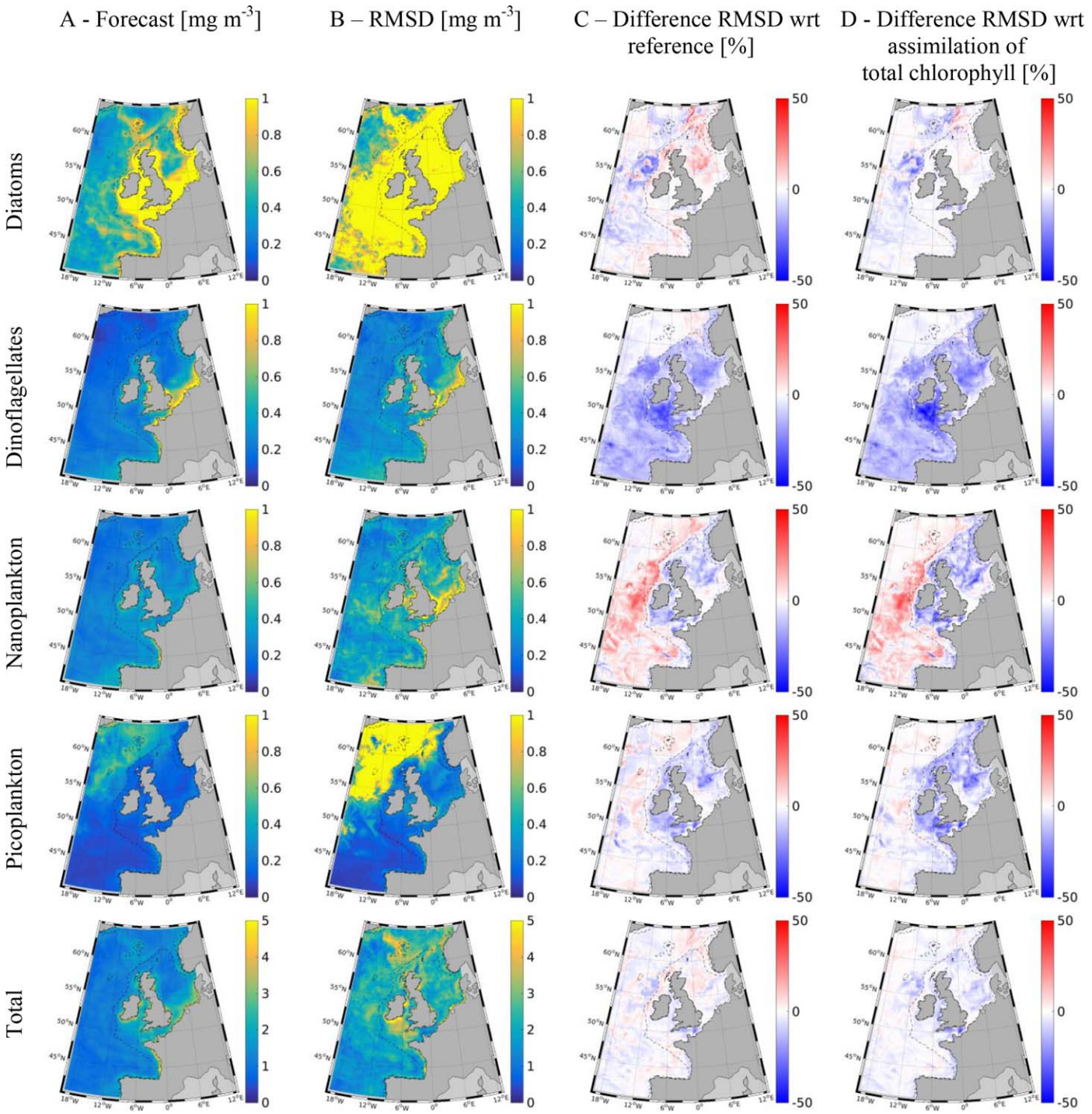

Figure 5. Skill of the PFT assimilation (forecast) in estimating the ocean-color chlorophyll concentrations of the four phytoplankton types and total phytoplankton: means in 1998–2003. Column (a) output of the PFT assimilative simulation; (b) root-mean-square-deviation (RMSD) between forecasts and ocean-color product; (c) percentage difference between the RMSD of the PFT assimilation and of the reference model without assimilation; and (d) percentage difference between the RMSD of the PFT assimilation and of the total chlorophyll assimilation.

The performance of the reanalysis for the in situ matchups of PFTs is substantially coherent with the results for the ocean-color product (Figures 5), though the number of available data is much lower. The reanalysis captures the ranges of diatoms, nanoplankton, and picoplankton, but the points are scattered around the bisector line, indicating that the high variability of these data was only partially represented by the

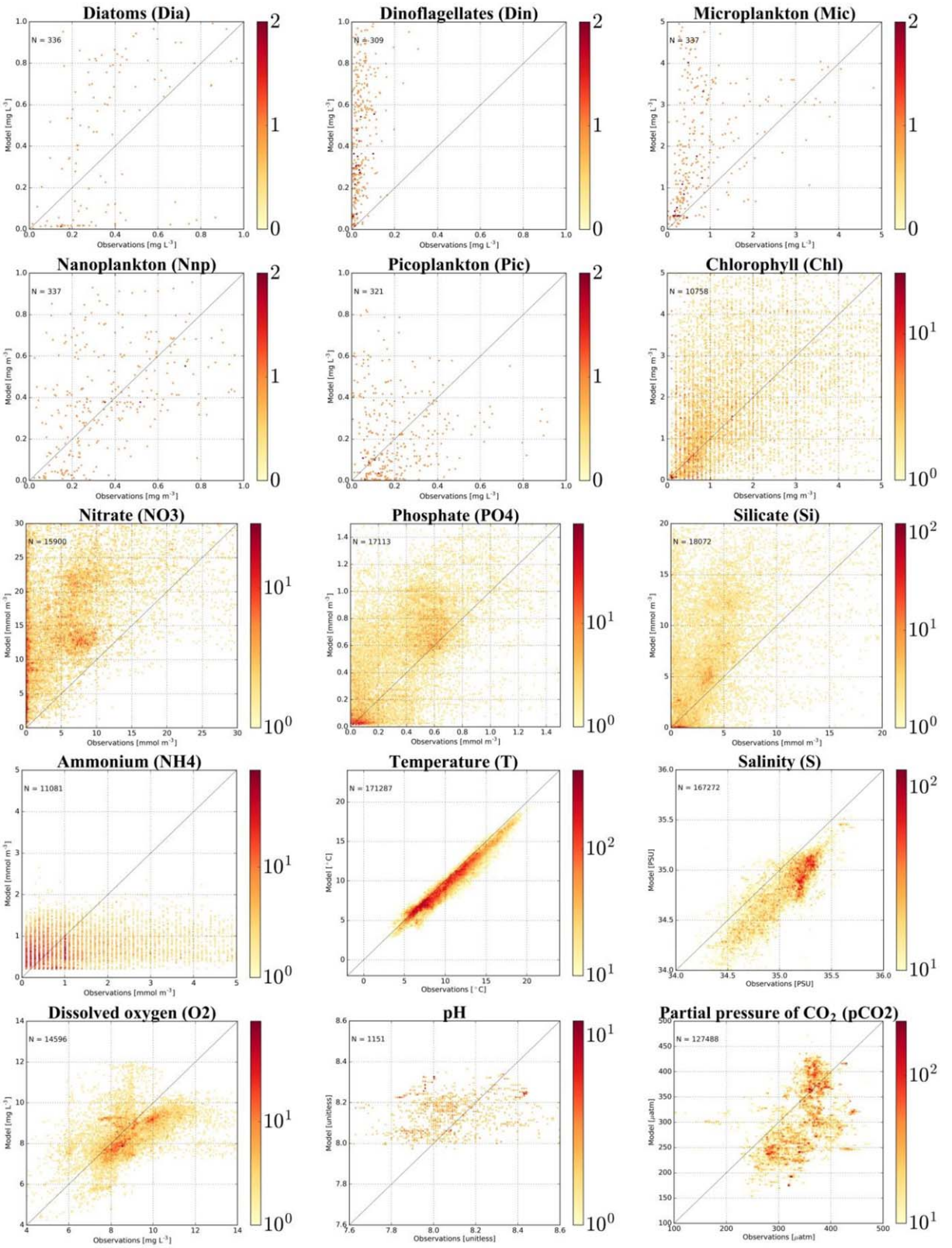

Figure 6. Density plots of the reanalysis output (*y* axis) versus in situ data (*x* axis) observed in the upper-shelf waters in the years 1998–2003. The colors represent the density in logarithmic scale, excepted the PFTs in linear scale; note the different ranges of the scales. N is the total number of match-ups.

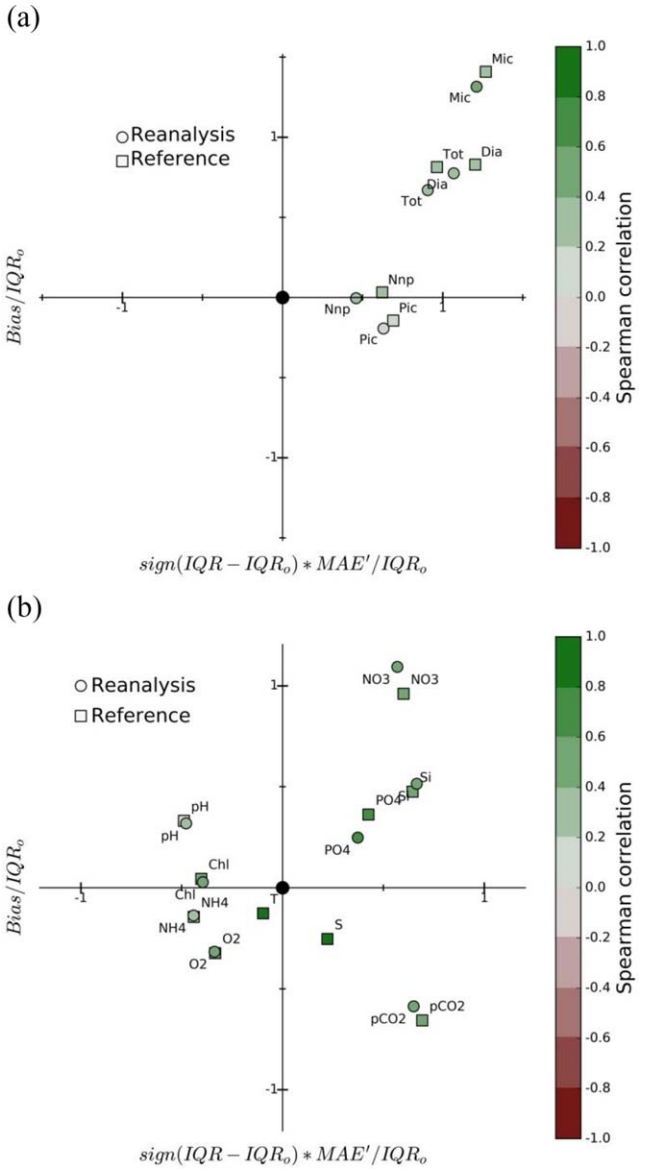

Figure 7. Skill of the reanalysis (circles) and reference (squares) simulations in estimating in situ data of plankton types (a) and of 10 physical and biogeochemical variables (b) observed in the upper-shelf waters in the years 1998–2003. The skills are shown in robust skill diagrams using metrics defined in section 2.4. The notation of the variables is defined in Figure 6.

reanalysis. Dinoflagellates are largely overestimated, as well as the whole microphytoplankton (sum of dinoflagellates and diatoms). The large spread of the match-ups of total chlorophyll from the ICES data set reflects the challenge of predicting the variability of this variable.

Quantitative skill metrics demonstrate that assimilation of ocean-color improved markedly the model simulation of in situ data for all the PFTs, as well as of pCO_2 and phosphate (Figure 7). All the circles representing the reanalysis skill for these variables are distinctly closer to the target center than the reference squares, indicating a decrease in both the bias and median absolute error (but only MAE′ decreased for picoplankton). Improvements in the individual PFTs drove a better estimate of total chlorophyll observations in the TOSCA data set (Tot in Figure 7a), which is only marginally evident for the much larger ICES data set (Chl in Figure 7b).

The reanalysis also increased clearly the bias of nitrate and, slightly, of silicate. The skill for the remaining variables was affected only negligibly (i.e., pH, O2, NH4). Temperature and salinity were not included in the analysis, though their good reference skill is reported for completeness.

The results presented here refer to the upper-shelf waters (section 2.4). The values of the skill metrics, as well as the impact of assimilation, were smaller in all other areas of the model domain (see supporting information Figure S1). The lower number of in situ data available for the open-ocean and deep waters, the limits of the course-resolution model in representing highly dynamic coastal waters (shallower than 10 m), and the limited ability of assimilating surface concentrations in correcting simulation at depth, are all factors leading to these results.

4. Discussion

4.1. Impact on the Simulation of the Plankton Community

Assimilation of ocean-color PFTs resulted in more realistic simulations of an emergent property of the ecosystem, such as the phytoplankton community structure of the North East Atlantic. Not only did the reanalysis improve the estimation of the individual PFTs from assimilated ocean color (Figures 4 and 5) and from semi-independent in situ observation (Figure 7), but it also improved the simulation of total chlorophyll, which was not an assimilated variable (Figures 4 and 5). In addition, the systematic corrections of the chlorophyll concentrations of both the individual PFT and total phytoplankton impacted an emergent property of the ecosystem, i.e., the relative fractions of the plankton groups defining the community structure, as one can see in Figure 8, derived from the results in Figures 4 and 5.

Assimilation improved the 1 month forecast of the observed community structure (Figure 8, column d) by keeping some memory of the marked improvements in the analysis steps (Figure 8, column c). Improvements were observed for all the four fractions of plankton types in large areas of the study region. This is also true for the fraction of nanoplankton in the ocean area (Figure 8), despite the absolute concentrations were deteriorated (Figures 4 and 5). The improved skill of the 1 month forecast (Figures 5 and 8d) was less obvious than the improvements in the analysis step (Figures 4 and 8c). In principle, the re-initialization of the assimilated variable toward the data should improve also the forecast of the next available data, with respect to the reference run. However, re-initialized biogeochemical states often tend to be "forgotten" and to converge back to the reference simulation because of the effect of hydrodynamics, forcing, boundaries values, and biogeochemical processes (Allen et al., 2003; Friedrichs et al., 2006; Teruzzi et al., 2014). In addition, multivariate analysis can produce values that are not consistent with the simulated model dynamics,

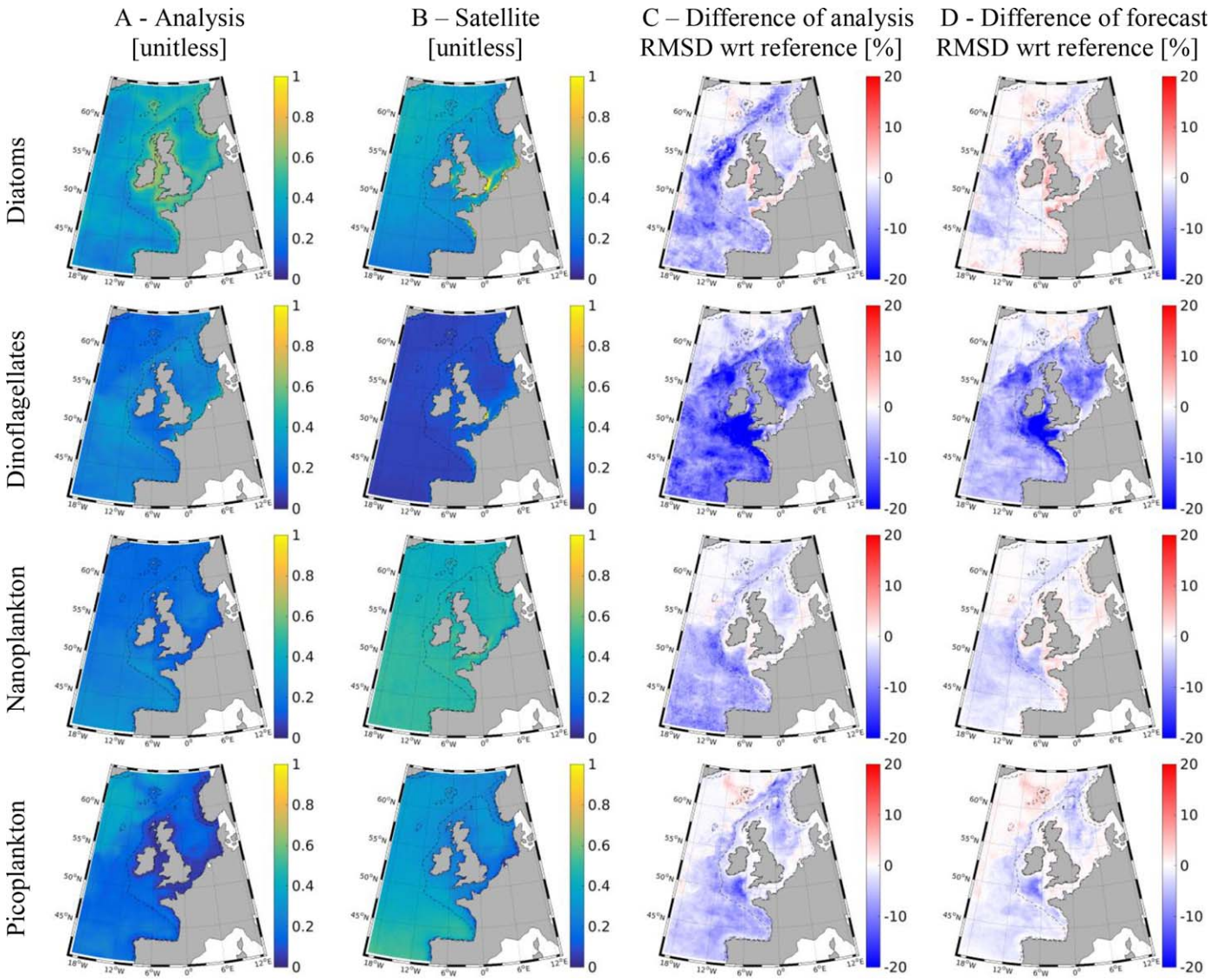

Figure 8. Skill of the PFT assimilation in estimating the plankton community structure derived from ocean-color. Column (a) PFT fractions from the assimilative analysis (computed from Figure 4); (b) PFTs fractions from the ocean-color product (computed from Figure 3); (c) percentage difference between the RMSD of the PFT assimilation (analysis) and of the reference model without assimilation; and (d) percentage difference between the RMSD of the PFT assimilation (forecast) and of the reference model without assimilation (from Figure 5).

e.g., outlier nutrient values, thus developing simulation instabilities that can lead the forecast to deteriorate both the assimilated and unassimilated variables (Ciavatta et al., 2011; Gregg et al., 2009). Here, these potential shortcomings of assimilation may explain why the forecast of the diatom fraction was slightly deteriorated in the North Sea (Figure 8), as well as the forecast of its absolute concentration (Figure 5). This is due to an increased production of diatoms fueled by the increased concentrations of nitrogen (see Figure 7), as discussed in section 4.2. Moreover, the reanalysis shifted the picoplankton relevance from South to North if compared to the satellite concentrations. The reanalysis also systematically underestimated the nanoplankton fraction and overestimated the fraction of dinoflagellate. The poor model simulation of dinoflagellates (see also Ciavatta et al., 2011) could be due to the fact that ERSEM does not represent key physiological traits specific to this group such as motility and the mixotrophic behavior (Flynn et al., 2012).

The relatively high errors associated with the PFT product, up to 100% (Figure 3), are comparable to the errors of the total chlorophyll products assimilated successfully in the region by Ciavatta et al. (2016), and certainly influenced the reanalysis of the plankton community presented here. Simplifying, in the EnKF

scheme, the higher the uncertainty in the observation, the smaller is the correction toward the assimilated data, for a fixed value of the model error. However, this did not prevent the scheme to correct substantially the predictions of the PFTs toward the bias-corrected product, most notably dinoflagellates that are characterized by the highest percentage error (Figure 3), and which are likely misrepresented by the model (Figures 6 and 7). The high error of the dinoflagellate satellite product is related to the complexity of separating this group from diatoms within the microplankton community (Brewin et al., 2017).

The effect of the uncertainty of the PFT product was evident also in the spatial variability of the assimilation skill in estimating the plankton community. In Figures 4, 5, and 8, assimilative improvements in the reference RMSD were in general smaller where the error of the assimilated PFT concentration was larger, i.e., in the coastal areas (Figure 3). Here the quality of satellite product is potentially deteriorated by resuspended sediments and colored dissolved organic matter discharged by rivers (Sathyendranath, 2000). Other error sources in the satellite-derived PFTs are described and discussed extensively by Brewin et al. (2017). In particular, they noted that their abundance-based algorithm infers the PFTs based only on semi-empirical relationships, parameterized using historical data sets. Therefore, the algorithm cannot detect abrupt blooms or long-term adaptive changes in the PFTs that deviate from the fixed relationships in the algorithm (Brewin et al., 2017). For such applications, the assimilation of PFT derived from spectral-based algorithms (e.g., Ciotti & Bricaud, 2006) are likely to be more preferable.

Assimilation of PFT outperformed the assimilation of total chlorophyll in estimating the plankton community (Figures 4 and 5). On the one side, this result follows the good performance of PFT assimilation in improving the estimation of the not-assimilated total concentration. However, this is also a consequence of the poor performance of total chlorophyll assimilation when performed with the new parameterization of ERSEM applied here (Butenschön et al., 2016), if compared to the application by Ciavatta et al. (2016) who used the previous parameterization by Blackford et al. (2004). The numerical experiment presented in Appendix A suggested that total chlorophyll assimilation performed poorly in Figures 4 and 5 because the new parameterization by Butenschön et al. (2016) enhanced nonlinearity between total chlorophyll and picoplankton (Figure A2), thus weakening the linear approximation and effectiveness of the Ensemble Kalman filter. In contrast, total chlorophyll assimilation was effective when the parameterization of the PFTs was more homogeneous and total chlorophyll was rather linearly proportional to the PFTs concentrations, as in Blackford et al. (2004) (Figure A2 in the Appendix A). Though the proportionality between total chlorophyll and PFTs allows total chlorophyll assimilation to be effective, it also implies that the corrections of the plankton community structure are unlikely (Ciavatta et al., 2011), in contrast with PFT assimilation proposed here.

Finally, we note that Xiao and Friedrichs (2014a) found less clear advantages in assimilating size-fractionated chlorophyll with respect to total chlorophyll for assimilative parameter optimization; however, the former product was preferable when assimilated simultaneously to particulate organic carbon. This suggests that simultaneous assimilation of ocean-color PFTs along with other biogeochemical and optical data from remote and in situ platforms, might be advantageous also in the context of sequential state-estimation with three-dimensional models.

4.2. Impact on the Simulation of Biogeochemical Variables and Fluxes

The reanalysis improved the simulation of relevant biogeochemical indicators (i.e., pCO_2 and phosphate) though some others were deteriorated (i.e., nitrate and silicate) (Figure 7). In our assimilative simulation, changes in the values of not-assimilated variables are caused by their direct corrections (i.e., increments) in the multivariate analysis steps of the EnKF (see section 2.2). In addition, the analysis increments can fuel the emergence of ecosystem properties during the forecast step, i.e., shifts in the simulated biogeochemical fluxes. These shifts can contribute to changes in the simulation of not-assimilated variables. These feedbacks of PFT assimilation are exemplified by the impact of the reanalysis on the simulations of the partial pressure of CO_2 (pCO_2, Figures 9 and 10) and nitrate concentration (Figure 11).

The reanalysis decreased the bias and the absolute errors of pCO_2 estimates (Figure 7) because it decreased their high reference values in the Irish Sea and in the English Channel, while it augmented the low values in the Bay of Biscay and in the Celtic Sea (Figure 9). This is due to indirect assimilative changes in the carbon fluxes (i.e., a decrease of the net community production in the Celtic Sea driven by the decreased plankton biomass, Figure 9) rather than by the negligible increments of dissolved inorganic carbon in the EnKF

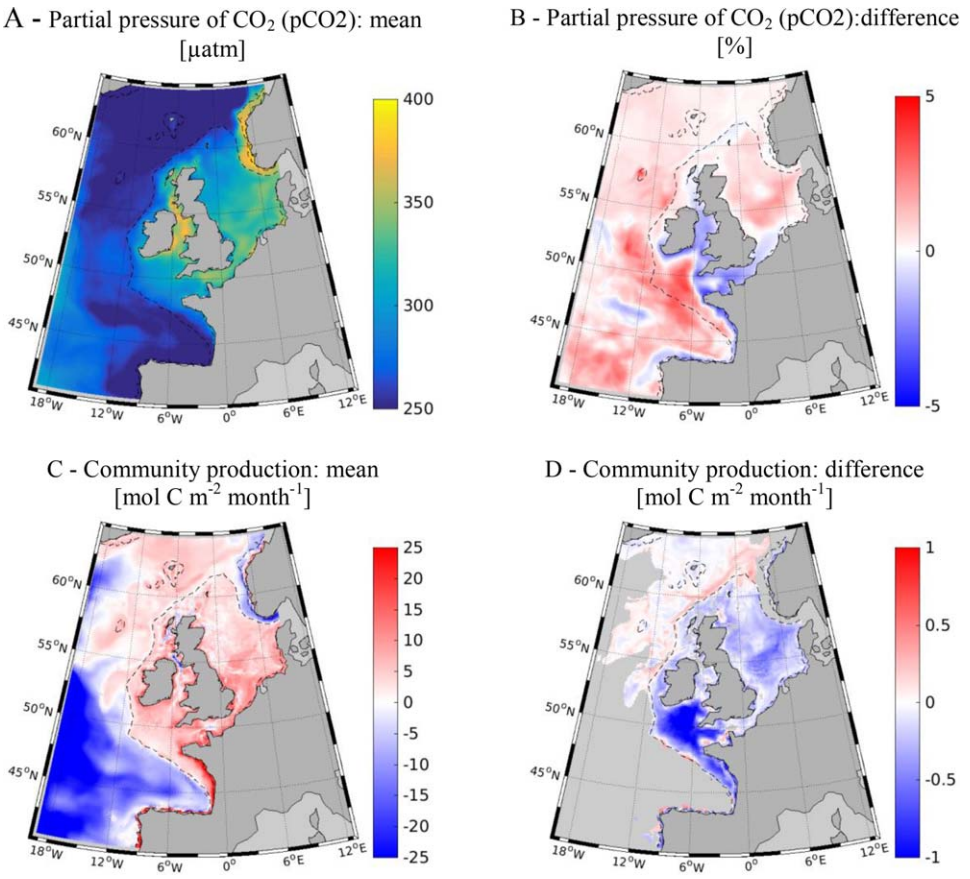

Figure 9. Reanalysis of pCO_2 (a and b; the partial pressure of CO_2) and of the net community production (c and d; the difference between the primary production and the respiration of phytoplankton, bacteria, and zooplankton). Mean values in the years 1998–2003 (a and c), and difference between the reanalysis and reference means (b and d). For the net community production, the difference was computed in the areas where both the reanalysis and reference means are positive, i.e., in the autotrophic areas of the study region.

analysis (not shown). As a relevant consequence, also the simulated air-sea fluxes of carbon dioxide changed in the reanalysis (Figure 10), following the patterns of its driver pCO_2 (Figure 9). The computed amount of atmospheric carbon taken up by the shelf-sea (54.4 TgC yr^{-1}, with a confidence range of 50–59 TgC yr^{-1} estimated by the 5th and 95th percentiles of the assimilative ensemble distribution) was only slightly different from the reference value of 53.5 TgC yr^{-1}. We note that the values computed here are higher than estimates obtained with previous versions of ERSEM (37.2–42 TgC yr^{-1} in Wakelin et al., 2012; 36–46 TgC yr^{-1} in Ciavatta et al., 2016), but this might also be due to an overestimation of the primary production (suggested by an overestimation of chlorophyll) caused by our overestimation of nitrate.

The reanalysis increased the bias of the nitrate estimates (Figure 7) because it increased the relative high concentrations of this nutrient in the North Sea and North West of Ireland, up to 20% (Figures 11a and 11b). Positive increments of nitrate are mainly responsible for this behavior (Figure 11c). However, the incremented nitrate also boosted the uptake of nitrate by phytoplankton (Figure 11d). In fact, in the model equations, enrichment in nitrate increases both the diatom production and the diatom uptake of nitrate itself (Butenschön et al., 2016). This implies that the forecast of diatoms degraded (Figure 5), but also that the nitrate uptake by total phytoplankton increased, despite the overall biomass of plankton decreased. This feedback of the model mitigated the impact of the positive increments of nitrate happened in the analysis steps.

We note that the deterioration of not-assimilated nutrients can occur when assimilating ocean color (see e.g., the discussions in Ford and Barciela, 2017; Teruzzi et al., 2014; Tsiaras et al., 2017), in particular when model issues lead the simulation to overestimate systematically both the phytoplankton biomass and the nutrient concentrations (Gregg et al., 2009), as it happened in our application for nitrate (Figure 7). The

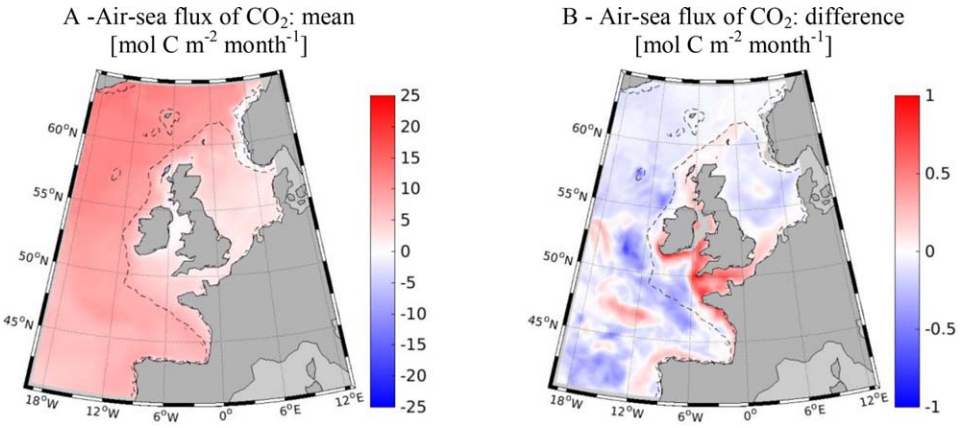

Figure 10. (a) Reanalysis of the air-sea flux of carbon dioxide and (b) difference with respect to the reference simulation. The differences were computed excluding the source areas, i.e., where either the reanalysis of the reference fluxes had negative values (e.g., in the Irish Sea).

overestimation of nitrate in the North East Atlantic is a recurrent feature of the POLCOMS-ERSEM model applied here, in particular in summer and in the coastal region (e.g., Butenschön et al., 2016; Ciavatta et al., 2016; Wakelin et al., 2012). Artioli et al. (2012) discussed possible causes of these weakness and they might also apply to our case: overestimation of benthic fluxes, underestimation of vertical mixing, overestimation

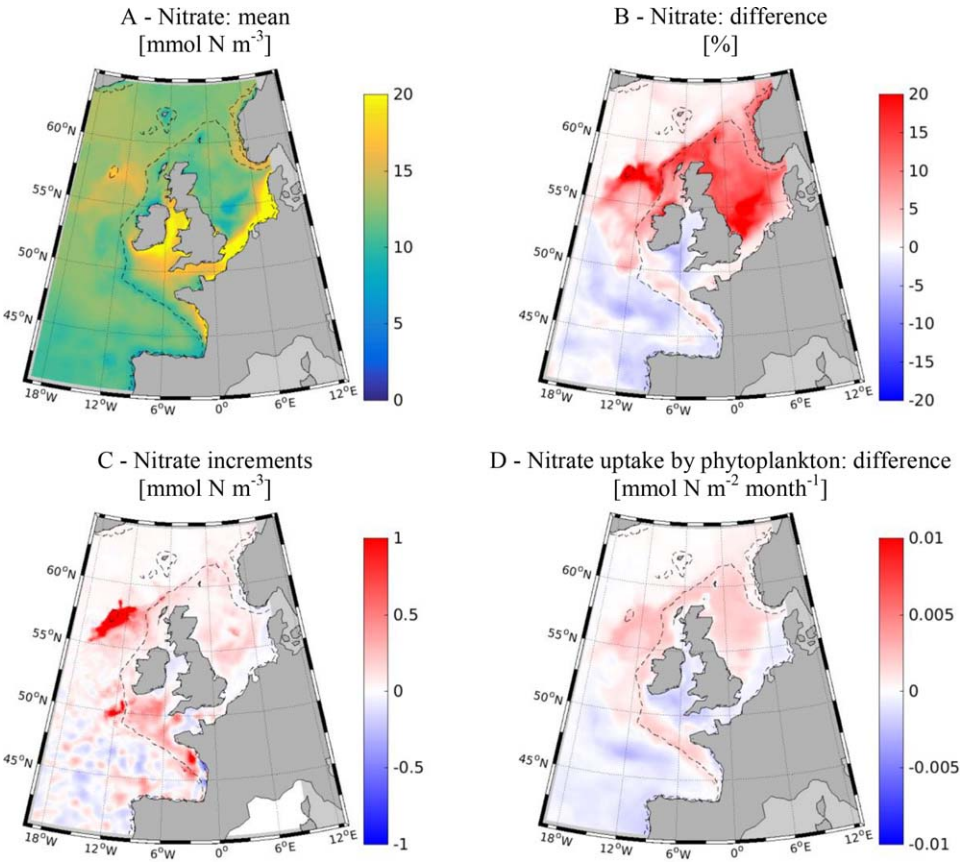

Figure 11. Impact of PFT assimilation on nitrate; (a) Mean reanalysis values in surface waters (up to 50 m); (b) Percentage differences of the reanalysis and reference mean values; (c) mean values of the EnKF analysis increments in the surface layer; and (d) mean value of the difference of the nitrate uptake by phytoplankton in the reanalysis and in the reference simulations.

of inputs from the North Sea rivers and the Baltic Sea. The latter weakness might be aggravated here by using climatological riverine data which do not represent the interannual variability of the inputs. Finally, we note that our simultaneous overestimation of nitrate and underestimation of ammonium suggests that the simplistic formulation of nitrification, which does not represent explicitly nitrifying prokaryotes, could be also a source of error. Despite these limits, the model was applied successfully in nutrient-focused applications, e.g., to assess eutrophication after linear correction of the nutrient output (Saux-Picart et al., 2015), and to compare impacts of oceanic nutrient inputs on primary production (Holt et al., 2012). Though we consider the model suitable to compare also data assimilation strategies in this context, we highlight that a comprehensive assessment of each of the nitrogen fluxes in the model need to be performed in future studies, given the clear importance of the nitrogen cycle in shelf seas.

5. Conclusions

The assimilation of plankton functional types from ocean color is a successful new approach to improve the simulation of ecosystem indicators, emergent properties (e.g., plankton community structure), and biogeochemical fluxes in shelf seas. Though in our application it deteriorated the simulation of some variables that were already overestimated by the model (e.g., nitrate), it also triggered a reaction of the simulated ecosystem to mitigate damages (e.g., the plankton uptake of nitrogen was increased).

Despite the advantages of the method, we stress that assimilation must not bypass much needed research to improve the understanding and representation of plankton functional types and related biogeochemical process in marine models (Shimoda & Arhonditsis, 2016). For example, we highlighted the benefit of enhancing differences among plankton types in the parameterization of ERSEM (Butenschön et al., 2016) to simulate a nonlinear link between picoplankton concentration and total chlorophyll that agrees with literature evidence (Brewin et al., 2017; de Mora et al., 2016). However, our application also pointed out that a rather simple proportionality still persists between total chlorophyll and diatoms in the ecosystem model, suggesting the need to better represent this highly diverse group (Polimene et al., 2014). Our results showed also that dinoflagellates are still poorly represented in ERSEM, indicating that the improvement of the formulation describing this group (e.g., the parameterization of the mixothrophic feeding behavior) is a priority.

Assimilation of PFTs outperformed the more traditional assimilation of ocean-color total chlorophyll because it simulated better the plankton community structure. In our application, this outcome might be also related to the use of the PFT parameterization by Butenschön et al. (2016), which enhanced the nonlinear relationships between some PFTs and total chlorophyll in ERSEM. However, a systematic comparison of the assimilation of the two ocean color products was outside the scope of this work and we recognize the utility of assimilating total chlorophyll with different parameterizations of ERSEM (e.g., Ciavatta et al., 2016) or different models (e.g., Ford & Barciela, 2017) or using assimilation methods that do not rely on linear assumptions, e.g., particle filters (e.g., Mattern et al., 2013).

The benefits of the approach rely on the quality of the size-class chlorophyll product that is available for assimilation. Here we used a product that was tailored to match the PFTs of ERSEM, calibrated and validated for the study region, and, crucially, provided with per-pixel estimates of bias and variance (Brewin et al., 2017). We anticipate that the development of ocean-color PFT algorithms, including the collection of in situ data for their validation (Bracher et al., 2017), will be boosted in the future for assimilation in other contexts (e.g., in the Mediterranean Sea; Di Cicco et al., 2017). We mention that also ocean-color products other than chlorophyll, e.g., optical properties (Ciavatta et al., 2014; Jones et al., 2016; Shulman et al., 2013) and particulate organic carbon (e.g., Xiao & Friedrichs, 2014a, 2014b) have proved useful for assimilation into marine models.

The novel approach proposed here is exportable to other PFT ecosystem models currently used to analyze biogeochemical fluxes in the global ocean (e.g., the models MEDUSA, Yool et al., 2013; NOBM, Rousseaux & Gregg, 2015; and MITgcm-biogeochemical model, Follows et al., 2007) or to predict biogeochemical indicators in shelf seas operationally (e.g., BFM, Teruzzi et al., 2014 and PISCES, Aumont et al., 2003), by adapting the assimilative operator that links the model PFTs to the ocean-color concentrations of plankton size-classes. The assessment of the method with an operational model of the North West European shelf

(NEMO-FABM-ERSEM) is the object of our ongoing work in the project "TOSCA" of the European Copernicus Marine Environment Monitoring Service (CMEMS).

Appendix A: Numerical Experiment With a Different PFT Parameterization

Here we show the results of a test simulation for year 1998 where ocean-color total chlorophyll was assimilated into a version of ERSEM with the PFTs parameterized as in Blackford et al. (2004) (see supporting information Table S1). The objective is to explain the poor performance of total chlorophyll assimilation in Figures 4 and 5, when using the novel parameterization by Butenschön et al. (2016).

We found that the assimilation of total chlorophyll using the Blackford et al. (2004) parameterization outperformed the assimilation of total chlorophyll with the Butenschön et al. (2016) parameterization (Figure A1), mainly because assimilation with Blackford et al. (2004) performed better in simulating picoplankton (Figure A1). Also the performance of the total chlorophyll assimilation for the other PFTs was slightly better with the Blackford et al. (2004) parameterization (in supporting information Figure S2).

This experiment suggested that total chlorophyll assimilation performed poorly in Figures 4 and 5 because the improved parameterization by Butenschön et al. (2016) enhanced nonlinearity between total chlorophyll and picoplankton (Figure A2), which was not evident in the simulation of other groups (see e.g., the relatively linear link between diatoms and total chlorophyll in supporting information Figures S3).

Such nonlinear-relationship, which is coherent with literature evidence (de Mora et al., 2016 and Brewin et al., 2017), may weaken the linear approximation of the Ensemble Kalman filter applied here, thus worsen his effectiveness when assimilating total chlorophyll with the Butenschön et al. (2016) parameterization.

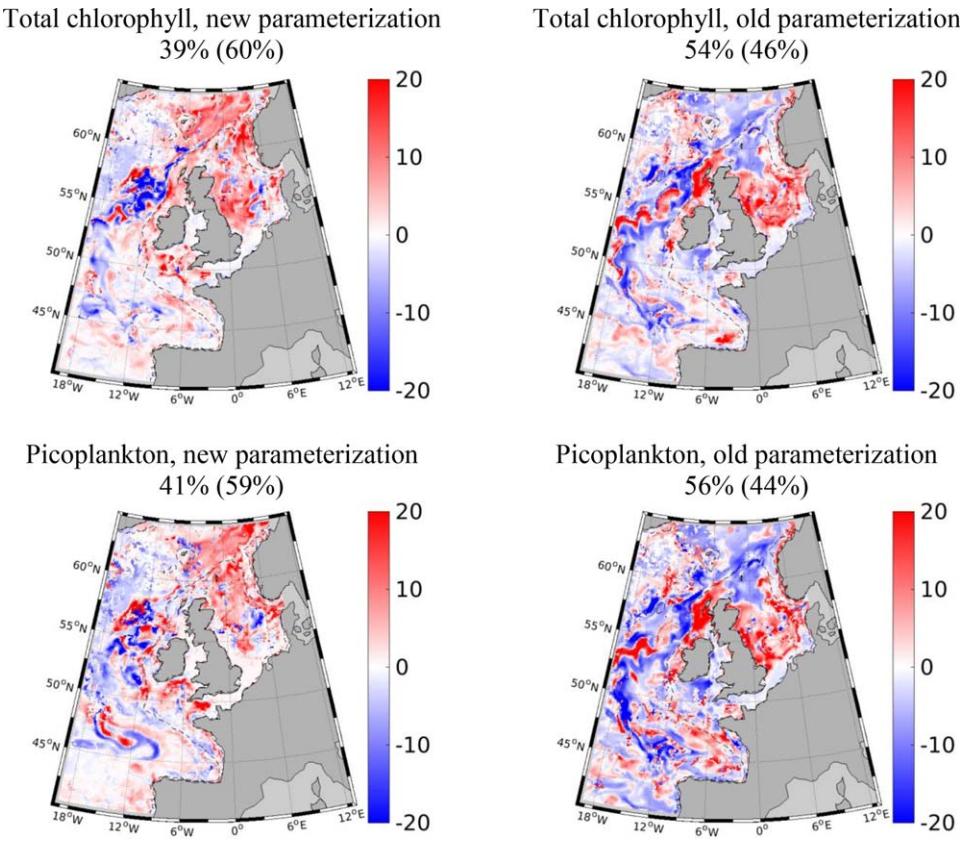

Figure A1. Percentage changes of reference RMSD when assimilating total chlorophyll using the (left) new and (right) previous parameterizations. (top plots) Chlorophyll and (bottom) picoplankton. The numbers in the titles of the maps indicate the percentage of the shelf area where assimilation improved (deteriorated) the reference simulation.

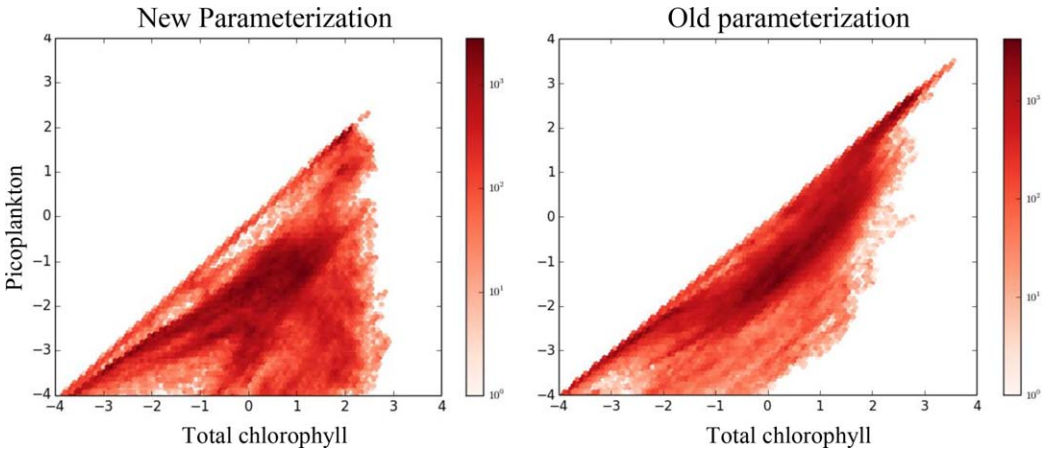

Figure A2. Density scatterplots of the log-transformed chlorophyll concentration of picoplankton versus total chlorophyll. The concentrations are ensembles forecasts in the assimilative simulations for year 1998 using the new (Butenschön et al., 2016) and previous (Blackford et al., 2004) parameterization of the PFTs in ERSEM. The linear correlation coefficients between picoplankton and total chlorophyll within the ensembles are 0.49 for the new parameterization and 0.93 for the previous one.

Acknowledgments
This work was carried out as part of the Copernicus Marine Environment Monitoring Service (CMEMS) project "Toward Operational Size-class Chlorophyll Assimilation (TOSCA)." CMEMS is implemented by MERCATOR OCEAN in the framework of a delegation agreement with the European Union. This work was also supported by the UK NERC through the National Centre for Earth Observation (NCEO), Modelling National Capability, the Atlantic BiogeoChemical (ABC) Fluxes Project of the RAPID-AMOC Programme, and by the EU H2020 project "TAPAS." This project has received funding from the European Union's Horizon 2020 research and innovation programme under grant agreement No 678396 (project TAPAS). We thank the European Space Agency's Climate Change Initiative—Ocean Color (http://www.esa-oceancolor-cci.org) for providing the ocean color data. The work used the UK National Supercomputing Service "ARCHER". The in situ data for validation were downloaded from the ICES database (http://ices.dk/marine-data) and Surface Ocean CO_2 Atlas (SOCAT) database (http://www.socat.info/). SOCAT is an international effort, endorsed by the International Ocean Carbon Coordination Project (IOCCP), the Surface Ocean Lower Atmosphere Study (SOLAS), and the Integrated Marine Biogeochemistry and Ecosystem Research program (IMBER), to deliver a uniformly quality-controlled surface ocean CO_2 database. In situ AMT data used were funded through the UK Natural Environment Research Council, through the UK marine research institutes' strategic research program Oceans 2025 awarded to PML and the National Oceanography Centre. This is contribution number 317 of the AMT program.

References

Allen, J. I., Eknes, M., & Evensen, G. (2003). An Ensemble Kalman filter with a complex marine ecosystem model: Hindcasting phytoplankton in the Cretan Sea. *Annales Geophysicae*, *21*(1), 399–411.

Allen, J. I., & Somerfield, P. J. (2009). A multivariate approach to model skill assessment. *Journal of Marine Systems*, *76*(1), 83–94.

Artioli, Y., Blackford, J. C., Butenschön, M., Holt, J. T., Wakelin, S. L., Thomas, H., et al. (2012). The carbonate system in the North Sea: Sensitivity and model validation. *Journal of Marine Systems*, *102*, 1–13.

Aumont, O., Maier-Reimer, E., Blain, S., & Monfray, P. (2003). An ecosystem model of the global ocean including Fe, Si, P colimitations. *Global Biogeochemical Cycles*, *17*(2), 1060. https://doi.org/10.1029/2001GB001745

Bakker, D. C., Pfeil, B., Smith, K., Hankin, S., Olsen, A., Alin, S. R., et al. (2014). An update to the Surface Ocean CO2 Atlas (SOCAT version 2). *Earth System Science Data*, *6*(1), 69–90.

Baretta, J. W., Ebenhöh, W., & Ruardij, P. (1995). The European regional seas ecosystem model, a complex marine ecosystem model. *Netherlands Journal of Sea Research*, *33*(3), 233–246.

Baretta-Bekker, J. G., Baretta, J. W., & Ebenhöh, W. (1997). Microbial dynamics in the marine ecosystem model ERSEM II with decoupled carbon assimilation and nutrient uptake. *Journal of Sea Research*, *38*, 195–211. https://doi.org/10.1016/S1385-1101(97)00052-X

Blackford, J. C. (1997). An analysis of benthic biological dynamics in a North Sea ecosystem model. *Journal of Sea Research*, *38*(3–4), 213–230.

Blackford, J. C., Allen, J. I., & Gilbert, F. J. (2004). Ecosystem dynamics at six contrasting sites: A generic modelling study. *Journal of Marine Systems*, *52*(1–4), 191–215. https://doi.org/10.1016/j.jmarsys.2004.02.004

Blackford, J. C., & Gilbert, F. J. (2007). pH variability and CO $_2$ induced acidification in the North Sea. *Journal of Marine Systems*, *64*(1), 229–241.

Borges, A. V. (2011). Present day carbon dioxide fluxes in the coastal ocean and possible feedbacks under global change. In P. Duarte & J. M. Santana-Casiano (Eds.), *Oceans and the atmospheric carbon content* (pp. 47–77). The Netherlands: Springer.

Bracher, A., Bouman, H., Brewin, R. J. W., Bricaud, A., Brotas, V., Ciotti, A. M., et al. (2017). Obtaining phytoplankton diversity from ocean color: A scientific roadmap for future development. *Frontiers in Marine Science*, *4*, 55. https://doi.org/10.3389/fmars.2017.00055

Brewin, R. J., Ciavatta, S., Sathyendranath, S., Jackson, T., Tilstone, G., Curran, K., . . . Dall'Olmo, G. (2017). Uncertainty in ocean-color estimates of chlorophyll for phytoplankton groups. *Frontiers in Marine Science*, *4*, 104.

Brewin, R. J., Sathyendranath, S., Hirata, T., Lavender, S. J., Barciela, R. M., & Hardman-Mountford, N. J. (2010). A three-component model of phytoplankton size class for the Atlantic Ocean. *Ecological Modelling*, *221*(11), 1472–1483.

Brewin, R. J., Sathyendranath, S., Jackson, T., Barlow, R., Brotas, V., Airs, R., & Lamont, T. (2015). Influence of light in the mixed-layer on the parameters of a three-component model of phytoplankton size class. *Remote Sensing of Environment*, *168*, 437–450.

Burchard, H., Holding, K., & Villareal, M. R. (1999). *GOTM, a general ocean turbulence model. Theory, applications and test cases* (Tech. Rep. EUR 18745 EN). Brussels, Belgium: European Commission.

Butenschön, M., Clark, J., Aldridge, J. N., Allen, J. I., Artioli, Y., Blackford, J., et al. (2016). ERSEM 15.06: a generic model for marine biogeochemistry and the ecosystem dynamics of the lower trophic levels. *Geoscientific Model Development*, *9*, 1293–1339. https://doi.org/10.5194/gmd-9-1293-2016

Christensen, O. B., Drews, M., Christensen, J. H., Dethloff, K., Ketelsen, K., Hebestadt, I., & Rinke, A. (2006). *The HIRHAM regional climate model, version 5* (DMI Tech. Rep. No. 06–17). Copenhagen, Denmark: DMI. Retrieved from http://www.dmi.dk/dmi/tr06-17.pdf

Chisholm, S. W. (1992). Phytoplankton size. In P. G. Falkowski & A. D. Woodhead *(Eds.), Primary productivity and biogeochemical cycles in the sea* (pp. 213–237). New York, NY: Springer.

Ciavatta, S., Kay, S., Saux-Picart, S., Butenschön, M., & Allen, J. I. (2016). Decadal reanalysis of biogeochemical indicators and fluxes in the North West European shelf-sea ecosystem. *Journal of Geophysical Research: Oceans*, *121*, 1824–1845. https://doi.org/10.1002/2015JC011496

Ciavatta, S., Torres, R., Martinez-Vicente, V., Smyth, T., Dall'olmo, G., Polimene, L., & Allen, J. I. (2014). Assimilation of remotely-sensed optical properties to improve marine biogeochemistry modelling. *Progress in Oceanography*, *127*, 74–95.

Ciavatta, S., Torres, R., Saux-Picart, S., & Allen, J. I. (2011). Can ocean color assimilation improve biogeochemical hindcasts in shelf seas? *Journal of Geophysical Research*, *116*, C12043. https://doi.org/10.1029/2011JC007219

Ciotti, A. M., & Bricaud, A. (2006). Retrievals of a size parameter for phytoplankton and spectral light absorption by colored detrital matter from water-leaving radiances at SeaWiFS channels in a continental shelf region off Brazil. *Limnology and Oceanography Methods*, *4*, 237–253. https://doi.org/10.4319/lom.2006.4.237

Daszykowski, M., Kaczmarek, K., Vander Heyden, Y., & Walczak, B. (2007). Robust statistics in data analysis—A review: Basic concepts. *Chemometrics and Intelligent Laboratory Systems*, *85*(2), 203–219.

Dee, D. P., Uppala, S. M., Simmons, A. J., Berrisford, P., Poli, P., Kobayashi, S., et al. (2011). The ERA-Interim reanalysis: Configuration and performance of the data assimilation system. *Quarterly Journal of the Royal Meteorological Society*, *137*(656), 553–597.

de Mora, L., Butenschön, M., & Allen, J. I. (2013). How should sparse marine *in situ* measurements be compared to a continuous model: An example. *Geoscientific Model Development*, *6*, 533–548.

de Mora, L., Butenschön, M., & Allen, J. I. (2016). The assessment of a global marine ecosystem model on the basis of emergent properties and ecosystem function: A case study with ERSEM. *Geoscientific Model Development*, *9*, 59–76. https://doi.org/10.5194/gmd-9-59-2016

Di Cicco, A., Sammartino, M., Marullo, S., & Santoleri, R. (2017). Regional empirical algorithms for an improved identification of Phytoplankton Functional Types and Size Classes in the Mediterranean Sea using satellite data. *Frontiers in Marine Science*, *4*, 126.

Evensen, G. (1994). Sequential data assimilation with a nonlinear quasi-geostrophic model using Monte-Carlo methods to forecast error statistics. *Journal of Geophysical Research*, *99*(C5), 10143–10162.

Evensen, G. (2003). The Ensemble Kalman filter: Theoretical formulation and practical implementation. *Ocean Dynamics*, *53*(4), 343–367. https://doi.org/10.1007/s10236-003-0036-9

Ferry, N., Parent, L., Garric, G., Drevillon, M., Desportes, C., Bricaud, C., & Hernandez, F. (2012). *Scientific Validation Report (ScVR) for reprocessed analysis and reanalysis MyOcean project report, MYO-WP04-ScCV-rea-MERCATOR-V1.0* (No. WP 04 – GLO – MERCATOR). Toulouse, France.

Flynn, K. J., Stoecker, D. K., Mitra, A., Raven, J. A., Glibert, P. M., Hansen, P. J., et al. (2012). Misuse of the phytoplankton–zooplankton dichotomy: The need to assign organisms as mixotrophs within plankton functional types. *Journal of Plankton Research*, *35*(1), 3–11.

Follows, M. J., Dutkiewicz, S., Grant, S., & Chisholm, S. W. (2007). Emergent biogeography of microbial communities in a model ocean. *Science*, *315*(5820), 1843–1846.

Ford, D., & Barciela, R. (2017). Global marine biogeochemical reanalyses assimilating two different sets of merged ocean colour products. *Remote Sensing of Environment*, *203*, 40–54. https://doi.org/10.1016/j.rse.2017.03.040

Ford, D. A., van der Molen, J., Hyder, K., Bacon, J., Barciela, R., Creach, V., et al. (2017). Observing and modelling phytoplankton community structure in the North Sea. *Biogeosciences*, *14*, 1419–1444. https://doi.org/10.5194/bg-14-1419-2017

Friedrichs, M. A. M., Hood, R. R., & Wiggert, J. D. (2006). Ecosystem model complexity versus physical forcing: Quantification of their relative impact with assimilated Arabian Sea data. *Deep Sea Research Part II: Topical Studies in Oceanography*, *53*(5–7), 576–600. https://doi.org/10.1016/j.dsr2.2006.01.026

Garcia, H. E., Locarnini, R. A., Boyer, T. P., & Antonov, J. I. (2006a). World Ocean Atlas 2005, Volume 3: Dissolved Oxygen, apparent oxygen utilization, and oxygen saturation. In S. Levitus (Ed.), *NOAA Atlas NESDIS 63*(p. 342). Washington, DC: U.S. Government Printing Office. Retrieved from https://www.nodc.noaa.gov/OC5/WOA05/pubwoa05.html

Garcia, H. E., Locarnini, R. A., Boyer, T. P., & Antonov, J. I. (2006b). World Ocean Atlas 2005, Volume 4: Nutrients (phosphate, nitrate, silicate). In S. Levitus (Ed.), *NOAA Atlas NESDIS 64*(p. 396). Washington, DC: U.S. Government Printing Office. Retrieved from https://www.nodc.noaa.gov/OC5/WOA05/pubwoa05.html

Gehlen, M., Barciela, R., Bertino, L., Brasseur, P., Butenschön, M., Chai, F., et al.. (2015). Building the capacity for forecasting marine biogeochemistry and ecosystems: Recent advances and future developments. *Journal of Operational Oceanography*, *8*(1), s168–s187.

Geider, R. J., MacIntyre, H. L., & Kana, T. M. (1997). Dynamic model of phytoplankton growth and acclimation: Responses of the balanced growth rate and the chlorophyll a: Carbon ratio to light, nutrient-limitation and temperature. *Marine Ecology Progress Series*, *148*(1–3), 187–200.

Gregg, W. W., Friedrichs, M. A. M., Robinson, A. R., Rose, K. A., Schlitzer, R., Thompson, K. R., & Doney, S. C. (2009). Skill assessment in ocean biological data assimilation. *Journal of Marine Systems*, *76*(1–2), 16–33. https://doi.org/10.1016/j.jmarsys.2008.05.006

Gregg, W. W., Ginoux, P., Schopf, P., & Casey, N. (2003). Phytoplankton and iron: Validation of a global three-dimensional ocean biogeochemical model. *Deep Sea Research Part II: Topical Studies in Oceanography*, *50*, 3143–3169.

Hansell, D. A. (2013). Recalcitrant dissolved organic carbon fractions. *Marine Science*, *5*, 421–445. https://doi.org/10.1146/annurev-marine-120710-100757

Holt, J. T., Butenschon, M., Wakelin, S. L., Artioli, Y., & Allen, J. I. (2012). Oceanic controls on the primary production of the northwest European continental shelf: Model experiments under recent past conditions and a potential future scenario. *Biogeosciences*, *9*, 97–117.

Holt, J. T., & James, I. D. (2001). An s coordinate density evolving model of the northwest European continental shelf - 1, Model description and density structure. *Journal of Geophysical Research*, *106*(C7), 14015–14034.

Holt, J. T., Proctor, R., Blackford, J. C., Allen, J. I., & Ashworth, M. (2004). Advective controls on primary production in the stratified western Irish Sea: An eddy-resolving model study. *Journal of Geophysical Research*, *109*, C05024. https://doi.org/10.1029/2003JC001951

Hu, J., Fennel, K., Mattern, J. P., & Wilkin, J. (2012). Data assimilation with a local Ensemble Kalman Filter applied to a three-dimensional biological model of the Middle Atlantic Bight. *Journal of Marine Systems*, *94*, 145–156.

Jackson, T., Sathyendranath, S., & Mélin, F. (2017). An improved optical classification scheme for the Ocean Colour Essential Climate Variable and its applications. *Remote Sensing of Environment*, *203*, 152–161. https://doi.org/10.1016/j.rse.2017.03.036

Jahnke,(2010). Global synthesis. In K.-K. Liu et al. (Eds.), *Carbon and nutrient fluxes in continental margins: A global synthesis, IGBP book series* (pp. 597–615). Berlin, Germany: Springer.

James, I. D. (1996). Advection schemes for shelf sea models. *Journal of Marine Systems*, *8*(3–4), 237–254. https://doi.org/10.1016/0924-7963(96)00008-5

Janjić, T., McLaughlin, D., Cohn, S. E., & Verlaan, M. (2014). Conservation of mass and preservation of positivity with ensemble-type Kalman Filter Algorithms. *Monthly Weather Review*, *142*(2).

Jolliff, J. K., Kindle, J. C., Shulman, I., Penta, B., Friedrichs, M. A., Helber, R., & Arnone, R. A. (2009). Summary diagrams for coupled hydrodynamic-ecosystem model skill assessment. *Journal of Marine Systems*, *76*(1), 64–82.

Jones, E. M., Baird, M. E., Mongin, M., Parslow, J., Skerratt, J., Lovell, J., et al. (2016). Use of remote-sensing reflectance to constrain a data assimilating marine biogeochemical model of the Great Barrier Reef. *Biogeosciences*, *13*(23), 6441.

Key, R. M., Kozyr, A., Sabine, C. L., Lee, K., Wanninkhof, R., Bullister, J. L., et al. (2004). A global ocean carbon climatology: Results from Global Data Analysis Project (GLODAP). *Global Biogeochemical Cycles*, *18*, GB4031. https://doi.org/10.1029/2004GB002247

Lahoz, W. A., & Schneider, P. (2014). Data assimilation: Making sense of earth observation. *Frontiers in Environmental Science*, *2*. https://doi.org/10.3389/fenvs.2014.00016

Le Quéré, C., Harrison, S. P., Colin Prentice, I., Buitenhuis, E. T., Aumont, O., Bopp, L., et al. (2005). Ecosystem dynamics based on plankton functional types for global ocean biogeochemistry models. *Global Change Biology*, *11*, 2016–2040. https://doi.org/10.1111/j.1365-2486.2005.1004.x

Lenhart, H. J., Mills, D. K., Baretta-Bekker, H., Van Leeuwen, S. M., Van Der Molen, J., Baretta, J. W., et al. (2010). Predicting the consequences of nutrient reduction on the eutrophication status of the North Sea. *Journal of Marine Systems*, *81*(1), 148–170.

Mattern, J. P., Dowd, M., & Fennel, K. (2013). Particle filter-based data assimilation for a three-dimensional biological ocean model and satellite observations. *Journal of Geophysical Research: Oceans*, *118*, 2746–2760. https://doi.org/10.1002/jgrc.20213

Mélin, F., Vantrepotte, V., Chuprin, A., Grant, M., Jackson, T., & Sathyendranath, S. (2017). Assessing the fitness-for-purpose of satellite multi-mission ocean color climate data records: A protocol applied to OC-CCI chlorophyll-a data. *Remote Sensing of Environment*, *203*, 139–151. https://doi.org/10.1016/j.rse.2017.03.039

Moore, T. S., Campbell, J. W., & Dowell, M. D. (2009). A class-based approach to characterizing and mapping the uncertainty of the MODIS ocean chlorophyll product. *Remote Sensing of Environment*, *113*(11), 2424–2430.

Natvik, L. J., & Evensen, G. (2003). Assimilation of ocean color data into a biochemical model of the North Atlantic - Part 1. Data assimilation experiments. *Journal of Marine Systems*, *40*, 127–153. https://doi.org/10.1016/s0924-7963(03)00016-2

Nerger, L., & Gregg, W. W. (2007). Assimilation of SeaWiFS data into a global ocean-biogeochemical model using a local SEIK filter. *Journal of Marine Systems*, *68*, 237–254. https://doi.org/10.1016/j.jmarsys.2006.11.009

Pätsch, J., & Lenhart, H. J. (2004). *Daily loads of nutrients, total alkalinity, dissolved inorganic carbon and dissolved organic carbon of the European continental rivers for the years 1977–2002, Berichte aus dem Zentrum für Meeres- und Klimaforschung/B: Ozeanographie* (Issue 48). Hamburg, Germany: Institut für Meereskunde, Zentrum für Meeres- und Klimaforschung. Retrieved from www.ifm.zmaw.de/fileadmin/files/theoretical_oceanography/Modelldaten_JP/RIVER.pdf

Pauly, D., Christensen, V., Guénette, S., Pitcher, T. J., Sumaila, U. R., Walters, C. J., et al. (2002). Towards sustainability in world fisheries. *Nature*, *418*, 689–695.

Polimene, L., Allen, J. I., & Zavatarelli, M. (2006). Model of interactions between dissolved organic carbon and bacteria in marine systems. *Aquatic Microbial Ecology*, *43*, 127–138.

Polimene, L., Brunet, C., Butenschön, M., Martinez-Vicente, V., Widdicombe, C., Torres, R., & Allen, J. I. (2014). Modelling a light-driven phytoplankton succession. *Journal of Plankton Research*, *36*(1), 214–229.

Reynolds, R. W., Smith, T. M., Liu, C., Chelton, D. B., Casey, K. S., & Schlax, M. G. (2007). Daily high-resolution-blended analyses for sea surface temperature. *Journal of Climate*, *20*, 5473–5496. https://doi.org/10.1175/2007JCLI1824.1

Rousseaux, C. S., & Gregg, W. W. (2015). Recent decadal trends in global phytoplankton composition. *Global Biogeochemical Cycles*, *29*, 1674–1688. https://doi.org/10.1002/2015GB005139

Sathyendranath, S. (2000*). Reports of the International Ocean-Color Coordinating Group* (Rep. 3, 140 p.). Dartmouth, Canada: IOCCG,.

Sathyendranath, S., Prieur, L., & Morel, A. (1989). A three-component model of ocean colour and its application to remote sensing of phytoplankton pigments in coastal waters. *International Journal of Remote Sensing*, *10*(8), 1373–1394.

Saux-Picart, S., Allen, J. I., Butenschön, M., Artioli, Y., de Mora, L., Wakelin, S., & Holt, J. (2015). What can ecosystem models tell us about the risk of eutrophication in the North Sea? *Climatic Change*, *132*(1), 111–125.

Saux-Picart, S., Butenschön, M., & Shutler, J. D. (2012). Wavelet-based spatial comparison technique for analysing and evaluating two-dimensional geophysical model fields. *Geoscientific Model Development*, *5*(1), 223–230.

Shimoda, Y., & Arhonditsis, G. B. (2016). Phytoplankton functional type modelling: Running before we can walk? A critical evaluation of the current state of knowledge. *Ecological Modelling*, *320*, 29–43.

Shulman, I., Frolov, S., Anderson, S., Penta, B., Gould, R., Sakalaukus, P., & Ladner, S. (2013). Impact of bio-optical data assimilation on short-term coupled physical, bio-optical model predictions. *Journal of Geophysical Research*, *118*, 2215–2230. https://doi.org/10.1002/jgrc.20177

Storto, A., Masina, S., & Dobricic, S. (2013). Ensemble spread-based assessment of observation impact: Application to a global ocean analysis system. *Quarterly Journal of the Royal Meteorological Society*, *139*(676), 1842–1862.

Teruzzi, A., Dobricic, S., Solidoro, C., & Cossarini, G. (2014). A 3-D variational assimilation scheme in coupled transport-biogeochemical models: Forecast of Mediterranean biogeochemical properties. *Journal of Geophysical Research*, *119*, 200–217. https://doi.org/10.1002/2013JC009277

Torres, R., Allen, J. I., & Figueiras, F. G. (2006). Sequential data assimilation in an upwelling influenced estuary. *Journal of Marine Systems*, *60*(3–4), 317–329. https://doi.org/10.1016/j.jmarsys.2006.02.001

Tørseth, K., Aas, W., Breivik, K., Fjæraa, A. M., Fiebig, M., Hjellbrekke, A. G., et al. (2012). Introduction to the European Monitoring and Evaluation Programme (EMEP) and observed atmospheric composition change during 1972–2009. *Atmospheric Chemistry and Physics*, *12*(12), 5447–5481.

Tsiaras, K. P., Hoteit, I., Kalaroni, S., Petihakis, G., & Triantafyllou, G. (2017). A hybrid ensemble-OI Kalman filter for efficient data assimilation into a 3-D biogeochemical model of the Mediterranean. *Ocean Dynamics*, *67*(6), 673–690.

Vichi, M., Pinardi, N., & Masina, S. (2007). A generalized model of pelagic biogeochemistry for the global ocean ecosystem. Part I: Theory. *Journal of Marine Systems*, *64*(1), 89–109.

Vörösmarty, C. J., Fekete, B., & Tucker, B. A. (1996). *River Discharge Database, version 1.0 (RivDIS v1.0), A contribution to IHP-V Theme 1. Technical documents in hydrology series* (Vol. 0–6.). Paris, France: UNESCO.

Wakelin, S. L., Holt, J. T., Blackford, J., Allen, J. I., Butenschön, M., & Artioli, Y. (2012). Modeling the carbon fluxes of the northwest European continental shelf: Validation and budgets. *Journal of Geophysical Research*, *117*, C05020. https://doi.org/10.1029/2011JC007402

Xiao, Y., & Friedrichs, M. A. M. (2014a). The assimilation of satellite-derived data into a one-dimensional lower trophic level marine ecosystem model. *Journal of Geophysical Research*, *119*, 2691–2712. https://doi.org/10.1002/2013JC009433

Xiao, Y., & Friedrichs, M. A. M. (2014b). Using biogeochemical data assimilation to assess the relative skill of multiple ecosystem models: Effects of increasing the complexity of the planktonic food web. *Biogeosciences*, *11*(11), 3015–3030.

Yool, A., Popova, E. E., & Anderson, T. R. (2013). MEDUSA-2.0: An intermediate complexity biogeochemical model of the marine carbon cycle for climate change and ocean acidification studies. *Geoscientific Model Development*, *6*, 1767–1811. https://doi.org/10.5194/gmd-6-1767-2013